This article has been accepted for publication in a future issue of this journal, but has not been fully edited. Content may change prior to final publication. Citation information: DOI 10.1109/COMST.2021.3111984, IEEE Communications Surveys & Tutorials

Underwater Optical Wireless Communications in Swarm Robotics: A Tutorial

Peter A. Hoeher[1], Jan Sticklus[2], and Andrej Harlakin[1]

[1]Faculty of Engineering, Kiel University, D-24143 Kiel, Germany
[2]GEOMAR Helmholtz Centre for Ocean Research Kiel, 24148 Kiel, Germany

***Abstract*—Underwater swarm robotics is an emerging topic. Compared to individual autonomous vehicles, high-capacity communication links are required between the mobile agents. In this tutorial, suitable communication technologies are studied, with emphasis on LED-based underwater optical wireless communications. A comprehensive overview about challenges, advances, and practical aspects of underwater swarm robotics employing optical wireless communications is provided. The tutorial includes the following topics: (1) Channel modeling fundamentals; (2) Physical layer transmission techniques for underwater optical wireless communications; (3) Data link layer aspects and hybrid transmission schemes; (4) Ambient light and interference suppression; and (5) Realization aspects. Finally, suggestions regarding future work are given. The tutorial is intended for readers with a background or interest in electrical and information engineering.**

***Index Terms*—Autonomous underwater vehicles, channel models, free-space optical communication, light emitting diodes, physical layer, swarm robotics, underwater communication, unmanned underwater vehicles, vehicular ad hoc networks, visible light communication.**

Abbreviations used Repeatedly

AlGaInP	Aluminum Gallium Indium Phosphide
ADC	Analog-to-Digital Converter
AMR	Anisotropic Magneto-Resistive
AOI	Angle of Incidence
AOP	Apparent Optical Property
APD	Avalanche Photo Diode
ARQ	Automatic Repeat Request
AUV	Autonomous Underwater Vehicle
BER	Bit Error Rate
CDOM	Colored Dissolved Organic Matter
CSIM	Constrained Superposition Intensity Modulation
DAC	Digital-to-Analog Converter
DCO-OFDM	Direct Current Optical OFDM
DD	Direct Detection
DEC	Decoder
DEM	Demodulator
DMT	Discrete Multitone Transmission
EM	Electro Magnetic
ENC	Encoder
FOV	Field of View
FSK	Frequency Shift Keying
FSO	Free Space Optical
FWHM	Full Width Half Maximum
IM	Intensity Modulation
InGaN	Indium Gallium Nitrite
IOP	Inherent Optical Property
IoUT	Internet of Underwater Things
LCD	Liquid-Crystal Display
LED	Light Emitting Diode
LOS	Line of Sight
MI	Magneto-Inductive
MIMO	Multiple-Input Multiple-Output
MISO	Multiple-Input Single-Output
MOD	Modulator
NAP	Non Algae Particles
NLOS	Non Line of Sight
OCDMA	Optical Code-Division Multiple-Access
OFDM	Orthogonal Frequency-Division Multiplexing
OOK	On-Off Keying
OWC	Optical Wireless Communication
PAM	Pulse Amplitude Modulation
PD	Photodetector
PHY	Physical Layer
PIN	Positive Intrinsic Negative
PPM	Pulse Position Modulation
PSK	Phase Shift Keying
PWM	Pulse Width Modulation
QAM	Quadrature Amplitude Modulation
QE	Quantum Efficiency
RF	Radio Frequency
RGB	Red Green Blue
Rx	Receiver
ROV	Remotely Operated Vehicle
SDMA	Space-Division Multiple Access
SIMO	Single-Input Multiple-Output
SISO	Single-Input Single-Output
SLAM	Simultaneous Localization and Mapping
SM	Superposition Modulation
SNR	Signal-to-Noise Ratio
SPF	Scattering Phase Function
TIA	Transimpedance Amplifier
Tx	Transmitter
UOWC	Underwater Optical Wireless Communication
UWC	Underwater Wireless Communication
VLC	Visible Light Communication
VSF	Volume Scattering Function

This article has been accepted for publication in a future issue of this journal, but has not been fully edited. Content may change prior to final publication. Citation information: DOI 10.1109/COMST.2021.3111984, IEEE Communications Surveys & Tutorials

I. Introduction

A. Background on AUVs and AUV Swarms

Robotics is a key technology for the maritime industry. Autonomous underwater vehicles (AUVs) are an impressively fast developing business. According to a recent financial analysis, the AUV market (without payload) is projected to expand from USD 638 million in 2020 to USD 1,638 million by 2025. It is expected to grow at a compound annual growth rate of 20.8 % from 2020 to 2025 [1].

The tasks of AUVs are manifold, and a swarm of AUVs (subsequently called "AUV swarm") provides even additional benefits [2]. AUVs are employed for commercial, scientific/oceanographic, environmental, and military/defense tasks. Among the commercial/service-oriented tasks are mapping and geophysical/archaeological surveying, monitoring and inspection of harbor basins, offshore constructions, and underwater pipelines, as well as search and salvage operations. Oil and gas industry are driving forces in the commercial segment. Scientific/oceanographic tasks include examinations of the entire water column, from the surface via the midwater regime to the deep-sea ocean. Examples include shallow water experiments on the one hand and seabed exploration on the other hand. Regarding environmental protection and monitoring applications, water quality sampling, habitat monitoring, baseline environmental assessments, debris/clearance surveys, fishery study, and emergency response are of great practical interest, for all types of water from lake to ocean. Border security and surveillance, antisubmarine warfare, monitoring smuggling of illegal goods, reconnaissance and exploration, and mine countermeasures are frequently mentioned military/defense tasks.

Most AUVs are employed in coastal waters, less in deep water. Small and midsize vehicles, called shallow AUVs (up to 100 meters depth rating) and medium AUVs (up to 1,000 meters depth), are most common. Actually, the number of large AUVs (more than 1,000 meters depth) and especially deep-sea AUVs (specified for up to 6,000 meters depth) is very limited. Currently, daily operations in conjunction with a supporting infrastructure (like an escorting boat or ship) are most frequent. In the near future, the amount of continuous-time operations is expected to grow, which is possible in conjunction with wireless power transfer. AUVs can be classified into two main groups: the torpedo-like type and the hovering capable type. The streamlined torpedo-like type is often used for areal mapping where the disadvantage of a stability-related minimum speed is less significant. The typically slower but better maneuverable hovering type is often applied for imaging purposes and inspection tasks.

AUV databases currently list over 1050 different underwater platforms from 350+ institutions [3], [4]. Among the elementary AUV equipment is a navigation unit (incl. compass, motion reference unit (MRU) or inertial navigation unit (INU), depth gauge, Doppler velocity log (DVL), and satellite navigation at the surface), a collision avoidance unit, a communication unit (incl. Wi-Fi, cellular and satellite radio at the surface, and underwater acoustic transceivers), a propulsion unit (incl. thrusters and thruster plus fin control), and a powerful battery module. The longterm position accuracy of inertial navigation systems is generally limited through drift of the accelerometers, but can be reduced by facilitating ultrashort baseline (USBL) systems or long baseline (LBL) transponder systems on the seafloor. Camera-based simultaneous localization and mapping (SLAM) represents an alternative solution. Beside the mentioned elementary equipment, task-specific sensors are usually installed, frequently side-scan or multibeam sonar, image and video cameras, conductivity, temperature, and depth (CTD) sensors, and other specialized sensors like sub-bottom profilers, magnetometers, and turbidity sensors. Since smaller vehicles are typically supposed for dedicated tasks and naturally provide a smaller volume, they are equipped with fewer sensors. This is due to fundamental weight/volume/bouyancy versus energy constraints, but also cost.

AUV swarms are a recent but emerging development [5]. Like their counterparts in terrestrial-based and air-based applications, called unmanned ground vehicles and unmanned aerial vehicles, AUV swarms are motivated by schools of fish, flocks of birds, and swarms of social insects. They are self-organizing systems. This requires intelligent processing within and communication skills between the swarm elements, which are subsequently referred to as agents or vehicles, respectively. AUV swarm design undoubtedly is an interdisciplinary area, including electronics, control, robotics, mechanical, navigation, communications, artificial intelligence, and oceanic engineering. Besides the challenges of AUV design, additional challenges arise such as swarm control, also referred to as flocking, path formation, aggregation, and object clustering.

Swarm intelligence principles can be applied to a number of different tasks. The entire group of AUVs can be used for problem solving [6]. Sometimes tasks can be parallelized and hence performed more efficiently and fast. Seabed mapping and water column monitoring are exemplary tasks matched to the capabilities of a heterogeneous swarm, since spatial sampling can be boosted significantly by swarm processing. In other applications, it may be more efficient to equip different agents with different sensors, referred to as a heterogeneous swarm. For example, a hovering-type of AUV could team-up with a torpedo-shaped AUV in order to benefit from their individual strengths and capabilities. Since power supply is a valuable resource, reducing the number of sensors per AUV is of great benefit. That way, cost can be reduced and mission time be increased. Some missions would fail if only a single AUV would be available. Furthermore, navigation skills are subject to improve in underwater swarms. Though individual position measurements are unreliable as mentioned before, by means of an exchange of localization data the precision can be enhanced for any agent. Additionally, AUV swarms can be used for relaying purposes: both data as well as energy can be exchanged contactlessly. Regarding data, selected AUVs may provide a bottle post service inside the communication network and to the surface. Such, almost arbitrary distances can be covered extending the communication range considerably. Similarly regarding energy, selected AUVs may serve as mobile power stations for other vehicles. Last but not least, due to redundancy, the outage is reduced and the failure rate

This article has been accepted for publication in a future issue of this journal, but has not been fully edited. Content may change prior to final publication. Citation information: DOI 10.1109/COMST.2021.3111984, IEEE Communications Surveys & Tutorials

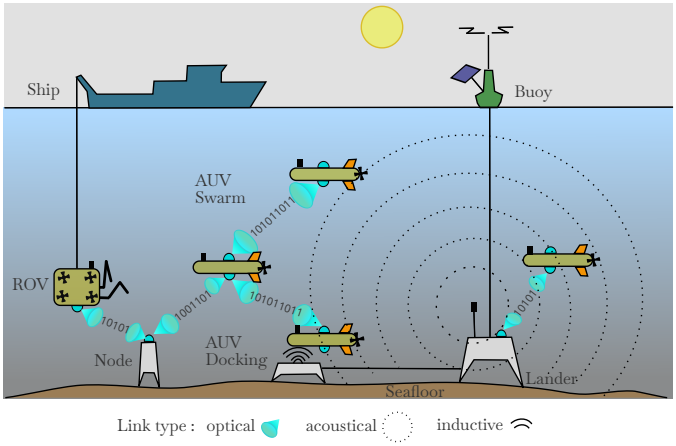

Fig. 1. Illustration of an underwater sensor network.

is improved, particularly in large swarms.

In any case, collaboration is a key recipe in swarm robotics. Against this background, the development of swarm robots with mobile, wireless communication infrastructure is necessary. Corresponding underwater wireless communication techniques and topologies will be studied next.

B. Communication Techniques in Underwater Swarm Robotics

A possible underwater sensor network is illustrated in Fig. 1. The network consists of fixed nodes like bottom landers and surface buoys, as well as mobile nodes like AUVs, remotely operated vehicles (ROVs), and ships. Sensors are attached to all types of nodes. The sensors are locally interconnected by a communication network. AUVs may be used as relays in this vehicular ad hoc network.

Most wireless underwater communication modems are based on sound waves [7]–[11]. Acoustic underwater communication is used between divers, ships and transponders, ships and underwater vehicles, in underwater sensor networks, etc. In effect, sound waves are the only resource enabling wireless underwater communication with medium (100 m to 1 km) and long range (1 km to a few 10 km) in seawater.

However, physical limitations of acoustic underwater communication are obvious. Acoustic modems are narrowband, which is caused by the limited bandwidth of commercial ultrasonic transducers as well as by multipath propagation. This restricts the achievable throughput. Data rates on the order of 100 bps to 100 Kbps are common, at long distances even less. Since the speed of sound is just about 1500 m/s, the propagation delay as well as the delay spread large. Due to a large propagation delay, communication protocols are difficult to establish. A large delay spread is troublesome with respect to intersymbol interference mitigation. Furthermore, the low (and variable) speed of sound is the reason for a fairly large Doppler spread. Hence, particularly in shallow waters and surf zones, data transmission is unreliable. For the same reason, mobility is problematic. Additionally, multi-user communication is difficult with acoustic modems due to bandwidth limitations and interference. The more transmitters are active, the less environmentally friendly sonar is. Also, sound waves typically do not travel in line-of-sight direction, hence acoustic localization is imprecise. Acoustic modems have been on the market for decades, and there is a wide range of products for various applications. This technology is considered reliable and proven in practice. In addition to communication, features such as positioning and networking are also available. Miniature versions are attainable for integration into vehicles. Power consumption is in the same order of magnitude as for optical systems. Despite the low bandwidth, these systems are indispensable due to their long range.

Underwater optical wireless communication (UOWC) is an alternative to acoustic modems at short distances. UOWC is an incidence of optical wireless communication (OWC) [12]–[19]. OWC can be classified as visible light communication (VLC) employing wavelengths in the visible range of the spectrum [20]–[25], and free-space optical (FSO) communication [26], typically using infrared (IR) laser links (Table I). In UOWC, only a small window of the visible light spectrum is useful. As the light velocity in seawater is about $2.25 \cdot 10^8$ m/s, i.e. three quarters of the light velocity in vacuum, the propagation delay is negligible. Much higher data rates are achievable compared to acoustic modems. Commercial light emitting diode (LED) based UOWC modems are currently offering up to 25 Mbps data rate, see Table IV in Section VI. Another advantage of light waves compared to sound is that precise distance measurements are possible, which is particularly important in AUV swarms.

TABLE I
COMPARISON OF LED-BASED UOWC WITH OUTDOOR FSO AND INDOOR VLC ("LI-FI").

Property	LED-based UOWC	Outdoor FSO	Indoor VLC
Light source	LEDs	Laser (typ.)	LEDs
Max. distance	10-50 m	Several 10 km	10 m
Max. data rate	250 Mbps	Several 10 Gbps	Several Gbps
Optical band	380-600 nm	800-1550 nm	380-720 nm
Challenges	Limited visibility	Scintillation	Ambient light
	Attenuation, scattering, refraction	Pointing & track.	Multipath
		Fog, rain	
Eye safety	No problem	Problematic	No problem

On the other side, there are some physical-related drawbacks of UOWC. Most critical is the communication range limitation caused by absorption and scattering. Visibility and range have a strong impact on the failure rate. Depending on the visibility, the communication range is limited to a few meters in harbor waters when using LEDs. Although in deep water and under ice data transmission in the 100 m range has been reported, UOWC can be classified as a near-range technique.

In principal, UOWC is not just possible with LEDs, but can also be based on lasers. Since laser beams are collimated, longer distances and higher data rates are feasible with lasers. With lasers, several 10 Gbps are achievable under lab conditions and at short communication distances, compared to several 100 Mbps achievable with LEDs. Concerning lasers, the pointing, acquisition and tracking problem of collimated laser beams must be solved though. In spatially fixed moorings

This article has been accepted for publication in a future issue of this journal, but has not been fully edited. Content may change prior to final publication. Citation information: DOI 10.1109/COMST.2021.3111984, IEEE Communications Surveys & Tutorials

this problem is easier to tackle. Since our focus is on AUV swarms and therefore on mobility, however, in the remainder only LED-based solutions will be explored. Regarding underwater laser communications, the interested reader is referred to [27]–[29] and related papers.

Besides ultrasonic and optical communication, electromagnetic waves sometimes are proposed for wireless underwater communication [30], [31]. Electromagnetic (EM) waves are radiated by antennas, i.e., the far-field regime $d \gg \lambda$ is of interest. With ultra long-wavelength radio (< 3 kHz) significant distances can be covered, at the expense of huge antenna sizes, low data rates, and high transmit powers, which is beyond the scope of AUV swarms. The low frequency ($30 - 300$ kHz), medium frequency ($0.3 - 3$ MHz), and high frequency ($3 - 30$ MHz) ranges are easier handable, but the attenuation of the medium increases with frequency in this regime. At radio frequencies used for cellular radio (> 800 MHz) and Wi-Fi ($2.4/5$ GHz), the penetration of electromagnetic waves in seawater is a few centimeters only [30]. For this reason, in shallow waters sometimes the air wave is exploited for range extension [31]. For the sake of completeness, it should be mentioned that although GHz radio frequency waves are not suitable as a communication medium for submerged AUVs, radio communication with an escort ship or satellites is frequently used when surfaced.

An alternative to electromagnetic waves is magneto-inductive (MI) communication, which is traditionally based on a modulated magnetic field emitted by a transmitter coil and picked-up by a receiver coil [32], [33]. Magneto-inductive communication operates in the near-field $d < \lambda$, i.e., in the non-radiating regime around the radiator. Hence, by definition MI communication is (like UOWC) a near-range technique. In the non-radiating regime, signal fading does not occur because waves cannot superimpose destructively. This is a distinctive difference compared to sound and EM waves. A decisive advantage magnetic fields have over acoustic waves is the high underwater propagation speed, which is similar to that of UOWC. Compared to UOWC, key advantages are the independence of visibility and the low sensitivity to water turbidity. MI communication is the only technology which is capable to simultaneously operate below and above the water surface or above and below the ground. The main disadvantage is the strong signal attenuation in salty water. Recently, in [34]–[36] a novel approach based on magnetic fields was proposed, where the receiver coil is replaced by a high-sensitivity wideband low-noise magnetic field detector, for instance an anisotropic magneto-resistive (AMR) sensor. Compared to conventional MI communication systems employing two coils, an additional advantage is that this family of sensors is small, lightweight, and offers a high bandwidth. This allows for a streamlined integration of both transmitter and receiver into the AUV, since the transmitter coil can also be integrated into non-metal hulls [35].

Electric currents have been proposed as an alternative to the use of EM or magnetic fields for digital underwater communications in [37]. Instead of antennas or coils, electrodes are used. This technology is bio-inspired by fish using weak electric fields for electrocommunication and sensing [38].

Since all mentioned wireless communication media have pros and cons, heterogeneous networking employing hybrid communication is a favourable strategy. For example, acoustic communication may serve as a wide-area umbrella cell, complemented by optical and/or MI communication in near-range links. Focus, however, will subsequently be on UOWC. Among all media suitable for wireless underwater communications, UOWC systems offer the largest bandwidth and channel capacity needed for high-speed communication in swarm networks [39], [40]. Besides UOWC between AUVs and between AUVs and underwater sensors, wireless light communication may also replace some of the cabling inside the AUV hull in order to save weight and cost.

C. Related Overview Articles

In the past five years, several esteemed surveys have been published in the field of underwater optical wireless communications [39]–[42], [29]. None of these contributions are classified as tutorials, however, and in none of these publications specific emphasis is on underwater swarm robotics.

In [39], the main focus is to understand the feasibility and the reliability of high data rate underwater optical links due to various propagation phenomena that impact the system performance. The paper provides an exhaustive overview of recent advances in UOWC recognizing the following aspects: (1) Channel characterization, modulation schemes, coding techniques, and various sources of noise which are specific to UOWC are discussed; (2) New ideas that promote future underwater communication systems are provided; (3) A hybrid approach to an acousto-optic communication system is presented that complements existing acoustic systems, resulting in high data rates, low latency, and energy-efficiency.

Reference [40] provides a comprehensive and exhaustive survey of state-of-the-art UOWC research considering three aspects: (1) Channel characterization; (2) Modulation; and (3) Channel coding techniques, together with practical implementation aspects of UOWC.

In [41], a comprehensive survey on the challenges, advances, and prospects of underwater optical wireless networks (UOWNs) from a layer by layer perspective is provided. The survey includes: (1) Physical layer issues including propagation characteristics, channel modeling, and modulation techniques; (2) Data link layer problems covering link configurations, link budgets, performance metrics, and multiple access schemes; (3) Network layer topics containing relaying techniques and potential routing algorithms; (4) Transport layer subjects such as connectivity, reliability, flow and congestion control; (5) Application layer goals; (6) Localization and its impacts on UOWN layers. Finally, open research challenges are outlined, and prospective directions for underwater optical wireless communications, networking, and localization studies are pointed out.

Reference [42] provides an overview on physical channel modeling as well as on current technologies and those potentially available soon. Particular attention is given to a literature survey, especially on the use of single-photon receivers.

The recent contribution [29] addresses various underwater challenges and offers insights into possible solutions. Focus is

This article has been accepted for publication in a future issue of this journal, but has not been fully edited. Content may change prior to final publication. Citation information: DOI 10.1109/COMST.2021.3111984, IEEE Communications Surveys & Tutorials

on laser-based UOWC systems. Novel solutions are proposed to ease the requirements on pointing, acquisition, and tracking for establishing robustness in UOWC links.

Besides these surveys specifically on UOWC techniques, several overview papers have been published on underwater wireless communications in general, including [43]–[45]. These contributions contain sections on UOWC.

D. Scope of this Tutorial

The objective of this tutorial is to provide a comprehensive overview of underwater optical wireless communication technologies that are suitable for use in agile robotic swarms. For this reason, only LED-based methods are taken into account since collimated laser beams suffer from the mentioned pointing, acquisition, and tracking problem. Compared to related surveys on underwater optical wireless communications, distinctive and partly novel contributions include the following aspects:

- Throughout this tutorial, OWC is tailored to underwater swarm robotics
- Application-oriented aspects of photonic devices are taken into account in channel modeling (II-B, II-C)
- Regarding the transmit signal design, the positive impact of large amplitude variations is highlighted (III-B)
- The concept of rectification is proposed in order to provide a framework regarding dimmable modulation schemes with just two amplitude levels and multicarrier modulation schemes (III-C, III-C)
- Constrained superposition intensity modulation is shown to be beneficial from implementation and power efficiency points of view (III-D)
- Optical frontends with single light source and multiple photodetectors are promoted (III-E)
- Hybrid communication is extended by magnetic inductance communication using wideband magnetic field detectors (IV-D)
- Properties of optical bandpass filters are studied for application in UOWC systems (V-A)
- Liquid crystal display (LCD) based ambient light and interference cancellation is considered in combination with underwater robots (V-B)
- The significance of pressure-neutral resin casting is emphasized (VI-A)
- The possibility of simultaneous illumination and communication is suggested for underwater camera recordings (VI-B)
- A market survey on underwater OWC modems is conducted (VI-C).

In Table II, a comparison between the surveys mentioned in Section I C and our contributions in this tutorial is provided.

E. Organization

The remainder of this tutorial is organized as follows: Section II deals with channel modeling. Besides the basic properties of the underwater optical channel, the impact of LEDs, photodetectors, as well as amplifiers are considered in conjunction with the channel characterization. In Section III, physical layer (PHY) transmission techniques are studied. Emphasis is on modulation schemes with just two amplitude levels, and on the superposition of square-wave signals. The time, frequency, and spatial domains are taken into account. The advantage of optical frontends employing multiple photodetectors rather than multiple light sources is highlighted. Since energy saving is of utmost importance, rate-adaptive and power-adaptive adaptation strategies are discovered. The section concludes with channel coding, equalization, and detection aspects. Data link layer aspects are studied in Section IV. Towards this goal, duplexing, multiuser, and multihop strategies are presented. Of special practical interest are hybrid transmission schemes, since underwater optical wireless communications is restricted to short ranges. Section V deals with ambient light and interference suppression – topics which are rarely considered in the underwater communications community so far. Focus is on optical bandpass-filter-based as well as on LCD-based techniques. In the latter case, the pixels of an LCD are used as an adaptive optical aperture. In Section VI, realization aspects are subsumed. The section starts with port and housing concepts, vehicular integration, and anti-biofouling ultraviolet illumination. Pressure-neutral resin casting is an advanced yet cheap housing technology that is particularly tailored to robotic swarms with small vehicles. Then, simultaneous illumination and communication/localization is discussed. The section closes with surveys on optical underwater modems and on underwater swarm projects. Finally, in Section VII conclusions are drawn, the lessons learned are highlighted, and an outlook on possible future research topics is provided.

II. Channel Modeling

A. Underwater Optical Channel Characterization

Underwater light propagation is a challenging scientific field because the optical properties of water are subject to strong variations. These depend on parameters such as the geographical location, the water depth, and the concentration of dissolved particles. In order to design reliable UOWC systems, it is therefore essential to develop an in-depth understanding of the most important parameters and their variability.

Optical properties of water are divided into two areas: inherent optical properties (IOP) and apparent optical properties (AOP). While IOPs solely depend on the medium itself, AOPs also depend on the structure of the light [46]. IOPs are described by two fundamental parameters: attenuation and scattering, which can be modeled as follows. Consider an incident light beam with wavelength λ and power P_i, which is passing a volume of water with thickness d. A portion P_a of light is absorbed, a fraction P_s is scattered, and the remaining portion P_t is passed. Conducting a limit value analysis of the absorbance $P_\mathrm{a}/P_\mathrm{i}$ with d approaching zero, one obtains the spectral absorption coefficient $a(\lambda)$. Analogous for the scatterance, $P_\mathrm{s}/P_\mathrm{i}$ yields the spectral scattering coefficient $b(\lambda)$. Both coefficients have the unit 1/m.

The spectral absorption coefficient $a(\lambda)$ is described as the sum of the following main absorbing constituents: $a_\mathrm{w}(\lambda)$ – absorption by the water itself, $a_\mathrm{phyt}(\lambda)$ – absorption by phytoplankton, $a_\mathrm{CDOM}(\lambda)$ – absorption by colored dissolved

This article has been accepted for publication in a future issue of this journal, but has not been fully edited. Content may change prior to final publication. Citation information: DOI 10.1109/COMST.2021.3111984, IEEE Communications Surveys & Tutorials

TABLE II
COMPARISON BETWEEN STATE-OF-THE-ART UOWC OVERVIEW PAPERS AND OUR CONTRIBUTIONS.

Topic	Kaushal et al. [39]	Zeng et al. [40]	Saeed et al. [41]	Spagnolo et al. [42]	This tutorial
Channel modeling	Theory-driven Turbulence, pointing	Theory-driven Turbulence	Theory-driven	Theory-driven	Application-oriented LED-based, no turbulence
Optical devices	na	na	na	Photodetectors	LEDs + photodetectors
Modulation	Classical schemes Single-carrier only	Classic schemes Single-carrier only	Classic schemes Single-carrier only	Classic schemes Single + multi-carrier	Novel schemes Single + multi-carrier
Multiple access	na	na	Considered	na	Considered
Network layer	na	na	Considered	na	na
Transport layer	na	na	Considered	na	na
Hybrid communication	Acoustic-optic	Acoustic-RF-optic	na	na	Magnetic-optic (+ acoust.)
Cooperative diversity	Relaying	na	na	na	Relaying
Interference cancellation	Opt. filter	na	Opt. filter	na	LCD-based + opt. filter
Optical head	Smart transceiver	Smart transceiver	na	na	Segmented head
Housing concepts	na	na	na	na	Included
Vehicular integration	na	na	na	na	Included
Illumination + commun.	na	na	na	na	Proposed
Localization	na	na	Considered	na	na
UOWC market survey	na	na	na	na	Conducted

organic matter, and $a_{\mathrm{NAP}}(\lambda)$ – absorption by non-algae particles or detritus. Absorption of pure seawater is mostly affected by molecular absorption of water molecules and less from dissolved salts. Compared to the other absorbing constituents, $a_{\mathrm{w}}(\lambda)$ strongly increases above $600\,\mathrm{nm}$ [47]. Phytoplankton, or in other words, chlorophyll-containing living microalgae, are typically mostly absorbing in the blue wavelength regime. The spectral absorption $a_{\mathrm{phyt}}(\lambda)$ depends on the natural variable mixture of species and on the chlorophyll concentration, which ranges from $0.1\,\mathrm{mg/m^3}$ in clear oceanic waters through up to $10\,\mathrm{mg/m^3}$ in coastal waters and $100\,\mathrm{mg/m^3}$ in lakes. Regarding the concentration modeling of chlorophyll, the interested reader is referred to [48]. Colored dissolved organic matter (CDOM), also known as Gelbstoff, is characterized on average by a main absorption in the UV and blue range and an exponentially decreasing absorption with increasing wavelength [49]. Finally, non-algae particles (NAP) or detritus, like debris of plankton and sediments, are showing a similar spectral trend as CDOM [50]. For better comparability, the spectral characteristics of the four absorbing constituents are depicted by means of two exemplary water types. The first, shown in Fig. 2, depicts the optical properties of the Atlantic Ocean. In a good approximation, these values correspond to oceanic water. The second example, shown in Fig. 3, depicts the properties of the Baltic Sea, which in turn is well approximated as coastal water. Generally, absorbing constituents, especially phytoplankton, underlie seasonal fluctuations and variations by the depth. The variability for different areas is presented in [51].

Scattering is the process when photons interacting with molecules or particles are forced to deviate from the straight trajectory. In channel modeling, scattering is described by the spectral scattering coefficient $b(\lambda)$, which is the sum of $b_{\mathrm{w}}(\lambda)$ - molecular scattering by the water itself and $b_{\mathrm{p}}(\lambda)$ - the scattering by particles. Scattering by turbulence is not considered here due to minor effects on short-range LED-based systems.

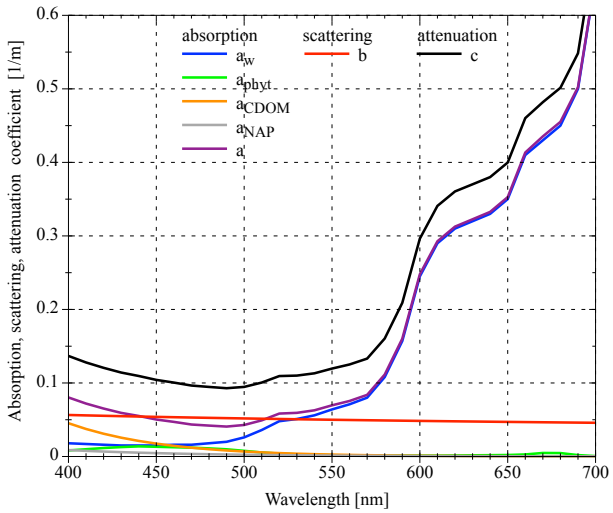

Fig. 2. This graphic depicts the modeled total spectral absorption $a(\lambda)$ and its constituents as well as the spectral scattering $b(\lambda)$ and the spectral attenuation $c(\lambda)$ exemplary for the Atlantic Ocean. Parameters are extracted from [51] and representing typical values for this area. (Sea water, chl=$0.2\,\mathrm{mg/m^3}$, $a_{\mathrm{CDOM}}(433)$=$0.02\,1/\mathrm{m}$ and S_{CDOM}=0.019 , $a_{\mathrm{NAP}}(433)$= $0.05\,1/\mathrm{m}$ and S_{NAP}=0.013).

On top of that, molecular scattering of the water can be neglected in most cases, as it will only contribute significantly under very clear oceanic conditions. Consequently, the overall scattering coefficient $b(\lambda)$ can be approximated by $b_{\mathrm{p}}(\lambda)$ representing scattering by organic and terrigenous particles. According to Haltrin [52], $b_{\mathrm{p}}(\lambda)$ can be modeled by one parameter, namely the chlorophyll concentration. As with the attenuation coefficient, the spectral scattering coefficient is plotted for two exemplary water types, i.e., the Atlantic Ocean, shown in Fig. 2, and the Baltic Sea, shown in Fig. 3.

A quantity, which describes the angular distribution of scattering, is the volume scattering function (VSF) $\beta(\lambda, \Psi)$. It can be interpreted as the "scattered intensity per unit inci-

This article has been accepted for publication in a future issue of this journal, but has not been fully edited. Content may change prior to final publication. Citation information: DOI 10.1109/COMST.2021.3111984, IEEE Communications Surveys & Tutorials

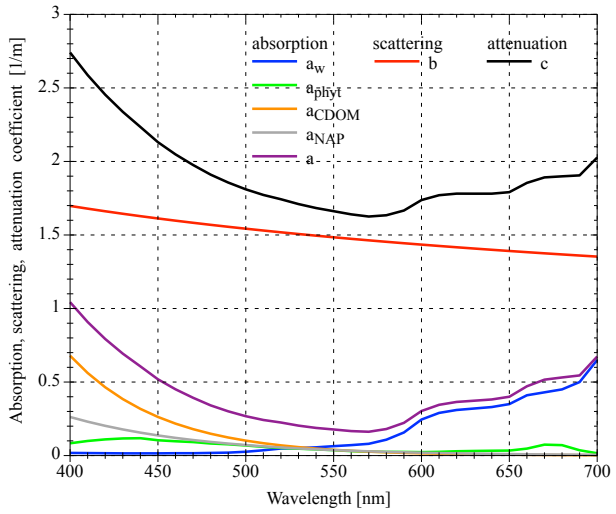

Fig. 3. This plot shows the modeled total spectral absorption $a(\lambda)$ and its constituents as well as the spectral scattering $b(\lambda)$ and the spectral attenuation $c(\lambda)$ exemplary for the Baltic Sea. Parameters are extracted from [51] and representing typical values for this area. (Sea water, chl=5 $\mathrm{mg/m^3}$, $a_{\mathrm{CDOM}}(433)$=0.3 1/m and S_{CDOM}=0.019 , $a_{\mathrm{NAP}}(433)$=0.15 1/m and S_{NAP}=0.013).

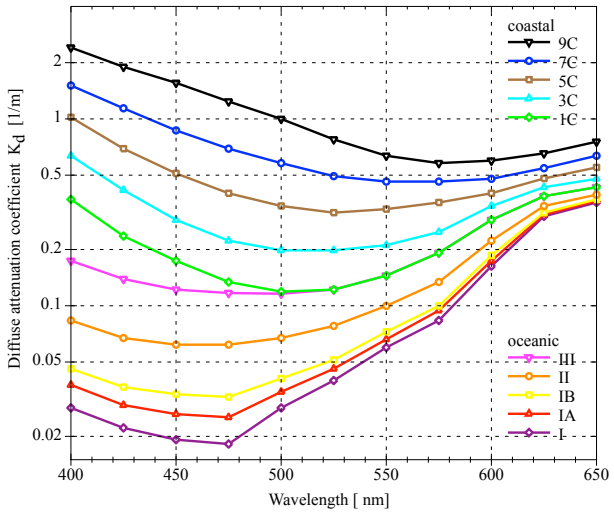

Fig. 4. Diffuse attenuation coefficient $K_{\mathrm{d}}(\lambda)$ as a function of wavelength λ for various oceanic and coastal water types according to the classification by N. G. Jerlov. Data is extracted from [56].

dent irradiance per unit volume of water" [46]. Normalizing this function with $b(\lambda)$ yields the scattering phase function (SPF) $\tilde{\beta}(\Psi, \lambda)$, which can be interpreted as the probability distribution of scattering as function of the scattering angle Ψ. The derivation is given in [46]. The main part of scattering occurs in forward directions at small angles Ψ. For numerical simulations, the SPF based on Petzold's measurements is widely used [53]. Alternative phase functions are introduced in [54]. The spectral beam attenuation coefficient $c(\lambda)$ is given as

$$c(\lambda) = a(\lambda) + b(\lambda). \tag{1}$$

Comparing the course of $c(\lambda)$ for the examples given in Fig. 2 and 3, it is observable that absorption is the main contributor of attenuation in oceanic water at higher wavelengths. Scattering, on the other hand, is the dominant contributor in coastal water.

The parameters introduced so far in this section have a strong impact on the path loss of underwater light propagation. Beer's law is a simple and widely used model for calculating the path loss:

$$P(d, \lambda) = P_0(\lambda) \cdot e^{-c(\lambda) \cdot d}, \tag{2}$$

where P_0 is the initial or transmitted power and $P(d, \lambda)$ is the residual power after traveling the distance d through the medium with wavelength λ. The application of (2) can lead to an underestimation of the received power, since it is only valid for collimated beams (i.e., laser beams) and scattered photons are excluded from consideration without the possibility of being scattered back to the path again. A classification of natural waters into water types was introduced by N. G. Jerlov in 1976. This classification differentiates five typical oceanic spectra I, IA, IB, II, and III, and five coastal spectra 1C, 3C, 5C, 7C, and 9C, from clear to more turbid, respectively (Fig. 4). To distinguish the water types according to Jerlov's classification, the downwelling diffuse attenuation coefficient $K_{\mathrm{d}}(\lambda)$ is measured, which represents an AOP. A suitable attenuation coefficient for the application of LED-based UOWC systems, denoted as $K_{\mathrm{sys}}(\lambda)$, is between $c(\lambda)$ and $K_{\mathrm{d}}(\lambda)$ [14].

The wavelength regimes, where the attenuation is smallest, depend on the particular water type. These wavelength regimes can be identified as blue to green for clear oceanic waters, shifting to green in clear coastal waters, and changing to yellow in turbid coastal waters. In very chlorophyll-rich harbour waters, the color may alter towards red. This behaviour is important in UOWC systems, because effectively an optical window is defined.

Optical turbulence is induced by salinity and temperature fluctuations of the ocean. Turbulence generates spatial changes of the refractive index. This causes intensity fluctuations of the propagating light, also known as scintillation. Laser-based UOWC is strongly affected by scintillation, while less collimated and shorter ranging LED-based systems are less affected [55].

B. Light Emitting Diodes

Even though the LED market is huge and diverse, the market share suitable for UOWC systems is comprehensive. This application is mainly limited to power or high-power semiconductor LEDs in the range of watts to tens of watts in the blue to amber color regime, equivalent to 450 nm to 600 nm wavelength. In this wavelength region, typically only three to five different colors are available, depending on the LED series. Examples of the spectral power distribution are given in Fig. 5. The spectra of the different colored LEDs are partly overlapping. Therefore, even in the case of using only blue, green, and amber LEDs, a separation into three independent physical channels can barely be achieved by optical bandpass filtering.

This article has been accepted for publication in a future issue of this journal, but has not been fully edited. Content may change prior to final publication. Citation information: DOI 10.1109/COMST.2021.3111984, IEEE Communications Surveys & Tutorials

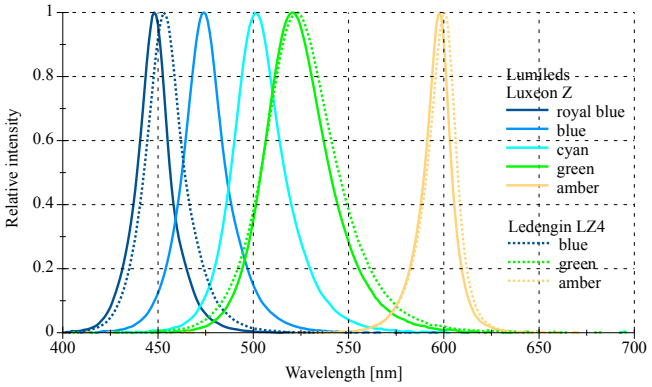

Fig. 5. Normalized spectral power distribution of two power LED series in the blue to amber color regime. Spectra were measured using Gigahertz Optics BTS256 for Lumileds Luxeon Z Series at I_f=350 mA and for Ledengin LZ4 series at I_f=700 mA, both at 25 °C.

Blue to green light is typically generated by indium gallium nitrite (InGaN) semiconductors, the spectral region from yellow to red by aluminum gallium indium phosphide (AlGaInP) [57]. The transition between these two bands, the so-called green-yellow gap of LEDs, is characterized by a low efficiency in terms of the ratio of emitted optical power to electrical power. The efficacy of green and yellow LEDs is currently only half or a third of that of blue or red LEDs. This feature of green and yellow LEDs is particularly disadvantageous for the use in coastal regions, as these waters just show the lowest attenuation in this wavelength area [58]. The market is offering higher-efficient alternatives, these are converted green or converted amber LEDs, which consist of high efficient blue LEDs combined with a phosphor conversion layer that converts blue to green respectively amber. One disadvantage of these converted color types is the significant higher linewidth, which hinders ambient light filtering. Another disadvantage is the longer rise and fall time in pulsed operation, reducing the bandwidth to only a few MHz, whereas direct color power LEDs are able to achieve tens of MHz bandwidth.

Planar-type power LEDs are offering a wide and smoothly decreasing radiation characteristic of 120° full width half maximum (FWHM) without optical beamforming. Therefore, in most cases, in UOWC there is a need to increase the irradiance through lenses or reflectors, which simultaneously leads to a reduction of the emission angle.

Over the last few years, micro LED arrays have been introduced as promising alternative. In experiments these efficient gallium nitride (GaN) based LEDs have demonstrated bandwidths up to 1 GHz [59]. Even though the emitted blue to cyan colored light has a very suitable wavelength for underwater applications, currently the achievable power is in the range of milliwatts. Micro LED arrays need further development and optimized optics before they can be used as a light source in future UOWC systems. A similar argument applies to other advanced LED technologies, for instance quantum-dot light emitting diodes (QLEDs).

In [60] the application of near ultraviolett (NUV) LED sources has been proposed for UOWC. Compared to the visible spectral range, solar irradiance decreases in this UV range, and thus tolerance to daylight improves, at the cost of increased absorption of water.

C. Photodetectors

A variety of photodetectors are suitable for high-speed communications and their proven operation in several experimental testbeds and different UOWC systems has been published in many places. Typical selection criteria are responsivity, active area, wavelength range, speed, and noise characteristics. Since these photodetectors exhibit distinct different characteristics, a closer look must be taken at the particular environmental and operational conditions. To establish a robust optical communication within a swarm of robots in coastal waters at daylight is clearly different from system performance test in a water basin and/or in a perfectly dark lab. Even though the responsivity of photodetectors is generally linear over many decades, the irradiance reaching the PDs active area is important for the decision about the type. For low-light high-speed applications the photomultiplier tube (PMT) and the silicon photomultiplier (SiPM) are generally appropriate. Utilizing these technologies in the dark clear ocean enables UOWC in the 100 m range for LED-based systems. But their individual drawbacks like high operating voltage and temperature sensitivity, noise, mechanical robustness, size, and cost needs to be taken into account. Nevertheless, SiPM detectors are a promising technology [61].

In comparison, positive intrinsic negative (PIN) PDs and avalanche PDs (APDs) are suitable for higher light levels occurring in real operations, like remaining ambient light after filtering in shallow waters and signal irradiances in short ranges of a few meters. Thus they are predestined for use in swarm robotics of the first generation, which unlikely takes place in the deep dark ocean. The different properties of both variants are discussed in more detail below (Fig. 6). PIN PDs are cheap and robust, but if the missing gain is compensated by large areas the increasing junction capacitance is reducing the speed. APDs with their internal gain are much faster, but need high reverse voltages to operate, are temperature sensitive, and noisier. The cost of large area PIN PDs and comparable APDs, due to the gain proportionally smaller sized, are in the same range.

As a special case of PDs, single-color LEDs can be operated as optical receiver and act similar to a photodiode [62]. This is particularly valid for high-power LEDs, since they have relatively large active areas comparable with medium-sized PDs. Another unique feature is the intrinsic bandpass filtering characteristic, combined with potential dual use as transmitting and receiving element it may be interesting in extraordinary applications or in the low-cost area.

D. Received Power

The interface between the optical domain and the electrical domain is given by the LED and the PD. The LED is converting electrical power into optical power, which is attenuated by the physical channel and finally converted back to electrical power by the PD and enhanced by an amplifier. Consequently,

This article has been accepted for publication in a future issue of this journal, but has not been fully edited. Content may change prior to final publication. Citation information: DOI 10.1109/COMST.2021.3111984, IEEE Communications Surveys & Tutorials

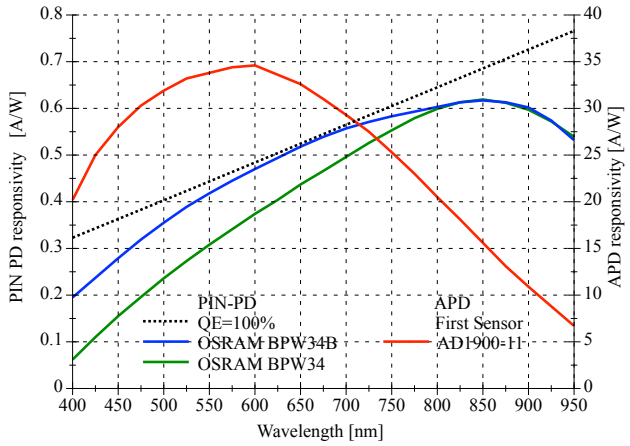

Fig. 6. Spectral responsivity of standard and blue enhanced PIN PDs as well as the quantum efficiency's (QE) theoretical maximum bound of QE=100 %. For comparison, the spectral development of an avalanche photodiode at a gain of M=100 is also shown. Data extracted from corresponding datasheets.

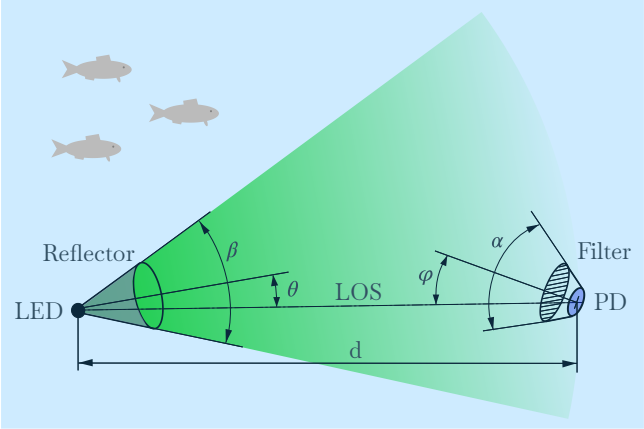

Fig. 7. Sketch of the optical domain of a UOWC system in line-of-sight configuration. At the transmitter side, the beam angle is denoted as β and the inclination by angle θ. Similarly at the receiver side, the field of view is denoted as α and the inclination by angle φ. LED and photodetector are separated by the distance d.

the electrical and optical power must be clearly distinguished, as well as the corresponding electrical and optical signal-to-noise ratios.

Line-of-sight (LOS) propagation happens if the light wave travels along the straight line between the source and the detector within the beam angle of the LED and the field of view (FOV) of the PD (Fig. 7). In LOS configuration, the transmitted power is attenuated by the square law and exponentially by Beer's law as given in (2). Additionally, the angular characteristic of the transmitter and receiver and their respective inclination need to be taken into account. In the optical domain, the received power can be written as [63], [64]

$$P_{\mathrm{R}} = P_{\mathrm{T}} \cdot GL \cdot f(\theta, \beta) \cdot \frac{A_{\mathrm{R}} \cos(\varphi)}{\pi d^2} \cdot e^{-c(\lambda) \cdot d} \qquad (3)$$

if $\varphi < \alpha$ and zero else, where P_T is the transmit power, θ the angle of irradiance, φ the angle incidence, β the beam angle, α the FOV of the photodetector, see Fig. 7, A_{R} the photo-

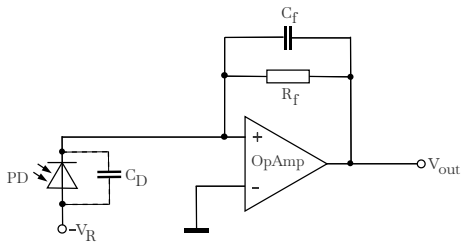

Fig. 8. Circuit diagram of a one-stage transimpedance amplifier as commonly used for PIN PDs and APDs. R_{f} and C_{f} are the feedback resistor and the feedback capacitor, respectively, and C_{D} represents the junction capacitance of the photodetector. V_{R} is the reverse voltage applied to reduce the capacitance of PIN-PDs, or to enable the avalanche effect in case of APDs.

sensitive area of the photodetector, and d the distance between transmitter (Tx) and receiver (Rx). The function $f(.,.)$ depends on the angle of irradiance and ~~on~~ the half-power angle of the light source. The parameter GL accounts for gain (e.g., due to collimating lenses) and loss (e.g., due to filtering) in the optical domain.

In non-line-of-sight (NLOS) propagation, the LOS path is either blocked by objects or lies outside the operating sectors of the LED or PD. The performance of scattering-based NLOS links has been investigated in [65], that of surface reflective NLOS links in [66] and [67].

E. TIA and Noise

Photocurrents generated by PIN PD and APD detectors are generally linear over many orders of magnitude, but very tiny. These currents, typically ranging from microamps to nanoamps in UOWC environments, are needing a transformation into voltages suitable for subsequent signal processing, primarily A/D conversion. This is commonly performed by one-stage and sometimes by two-stage transimpedance amplifiers (TIAs). One-stage TIAs mainly consist of an operational amplifier (OpAmp), a feedback resistor R_{f}, and a feedback capacitor C_{f}, as depicted in Fig. 8. The feedback resistor determines the amplification and the acceptable light level before saturation of the amplifier. The dimensioning of C_{f} must be done very carefully, because it has a significant influence on the stability, the impulse response, and the cut-off frequency. The required capacitance values are often in the range of a few picofarad, and the stray capacitances can be correspondingly significant, so it is advisable to make measurements in addition to simulations. Regarding the first TIA stage, two topologies are common: the photovoltaic mode and the photoconductive mode, respectively. In the photovoltaic mode, the reverse voltage V_{R} is set to be zero. Correspondingly, the PD is virtually short-circuited by the OpAmp. This has a positive impact on the noise figure. Therefore, the photovoltaic mode is useful for low-SNR applications. In the photoconductive mode, $V_{\mathrm{R}} > 0$. Consequently, the junction capacitance of the PD reduces because the effective gap between differently doped semiconductor layers increases. Consequently, the photoconductive mode is suitable for high-speed applications. APDs must always be operated with a high reverse voltage, otherwise the avalanche effect will not occur. Since many

This article has been accepted for publication in a future issue of this journal, but has not been fully edited. Content may change prior to final publication. Citation information: DOI 10.1109/COMST.2021.3111984, IEEE Communications Surveys & Tutorials

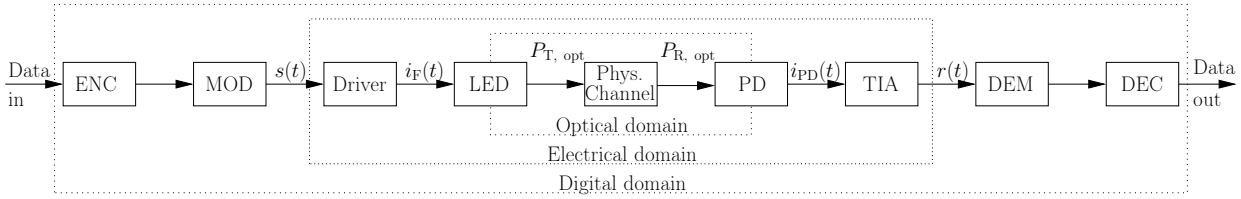

Fig. 9. Block diagram of a UOWC system. Note the distinction between the optical domain and the electrical domain.

variables have to be considered in designing a TIA circuit for the respective PD and light conditions, the use of a simulation tool is recommended, for instance [68].

The maximal achievable bit rate of a communication system, called channel capacity, linearly depends of the bandwidth and logarithmically on the signal to noise ratio (SNR). The SNR is the ratio between the average signal power at the demodulator input and the average noise power measured at the same point. As bandwidth-limiting factors, the following parameters can be identified: the rise/fall time of the LED source including the driver, and the junction capacitance of the PD including the TIA. For proper operation a certain bit error rate (BER) needs to be fulfilled. Depending on the applied modulation and channel coding scheme a particular SNR is required for the targeted BER. The most common modulation schemes need an SNR in the electrical domain roughly in the range of $10\,\mathrm{dB}$ to $20\,\mathrm{dB}$ for a targeted BER of 10^{-6} [25]. The received signal power is determined by the distance between Tx and Rx, the responsivity of the PD (measured in amperes per watt of received power), and the feedback resistor. The noise power is generally dominated by shot noise, thermal noise, and amplifier noise. Shot noise is caused by the photons of the desired light source as well as by ambient light. It depends on the responsivity of the PD and is bandwidth dependent. Thermal noise depends on the temperature, the feedback resistor, the bandwidth, and the responsivity of the PD. The amplifier noise needs to be considered in the noise examination as well. The corresponding parameters are the voltage noise density and the current noise density, which can be extracted from the amplifier's datasheet. For TIA applications, it is recommendable to identify low-noise amplifiers. At this point it becomes clear that the use of a simulation tool is essential to handle the plurality of variables. Generally, it can be remarked that the noise arising from the detector's dark current is negligible in most cases. Usually PIN-PD-based systems are more robust to ambient light conditions, but slower and less sensitive, whereas APD-based systems cope worse under ambient light conditions due to shot noise, but offer comparatively better sensitivity and higher speed.

III. Physical Layer Transmission Techniques

A. UOWC Transmission System

In Fig. 9, a block diagram of a UOWC system is depicted [64]. The task of the digital modulator (MOD) is to convert a bit stream into an analog waveform $s(t)$. The modulator is followed by an analog driver circuit. The forward current $i_{\mathrm{F}}(t)$ feeds the light source. A photodetector converts the received photons into a photocurrent $i_{\mathrm{PD}}(t)$. A transimpedance amplifier transforms the photocurrent into a voltage $r(t)$. Given the received signal $r(t)$, the demodulator (DEM) processes and delivers the recovered bit stream. Optionally, the bit stream is encoded by a channel encoder (ENC) and correspondingly decoded by a channel decoder (DEC).

B. Fundamentals on Intensity Modulation

Concerning the modulation scheme, we need to distinguish between coherent and non-coherent light sources. Lasers are able to emit coherent light waves. Therefore, two-dimensional modulation schemes, i.e. quadrature amplitude modulation (QAM) schemes, are implementable. The QAM constellation diagram consists of symbol points originating from two orthogonal pulse amplitude modulation (PAM) systems. Therefore, two statistically independent data streams may be transmitted simultaneously. In contrast to that, LEDs cause a spontaneous emission of photons, i.e., the phase is random and hence not useful for data transmission. As a consequence, only intensity modulation is implementable. Hence, LEDs impose two constraints: the transmit waveform $s(t)$ must be real-valued and non-negative, i.e., unipolar. For the first reason, the spectral efficiency (i.e., the number of bits per symbol that can be transmitted in a bandwidth of one Hertz) is degraded compared to laser communication. For the second reason, the transmit waveform is biased. Since a bias does not contribute to the detection performance, the power efficiency (i.e., the necessary SNR to fulfill a given quality constraint) is degraded as well. Intensity modulation (IM) is usually combined with direct detection (DD), dubbed IM/DD [12]–[19].

Particularly in mobile UOWC applications, the SNR at the demodulator input typically is limited and hence of primary concern. For this reason, any technique capable to improve the SNR is of interest. It has rarely been reported that amplitude variations of the transmit signal $s(t)$ should be as large as possible in order to maximize the received power in the electrical domain. This is the domain where data detection takes place at the receiver side. The average-power-to-squared-mean ratio κ is defined as the ratio between the average signal power and the squared mean value of the signal (Fig. 10). The average signal power is calculated as the expected value of the squared signal amplitudes. The squared mean, on the other hand, is calculated as the square of the expected value of the signal amplitudes. For the sake of clarity, Fig. 10 shows the square of both waveforms. κ is a pure signal property, similar to the more familiar peak-to-average power ratio. The larger the amplitude fluctuations, the larger this ratio κ is. It can be proven that the received power in the electrical

This article has been accepted for publication in a future issue of this journal, but has not been fully edited. Content may change prior to final publication. Citation information: DOI 10.1109/COMST.2021.3111984, IEEE Communications Surveys & Tutorials

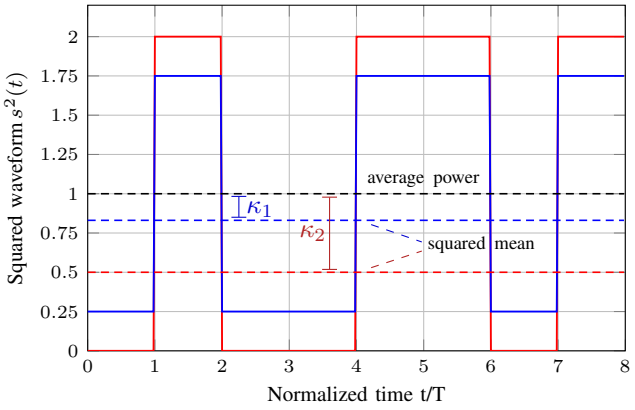

Fig. 10. Definition of the average-power-to-squared-mean ratio κ given two different waveforms. An OOK signal is represented by red color, and a binary PAM signal by blue color. The former waveform is superior from an SNR point of view, given the same average signal power.

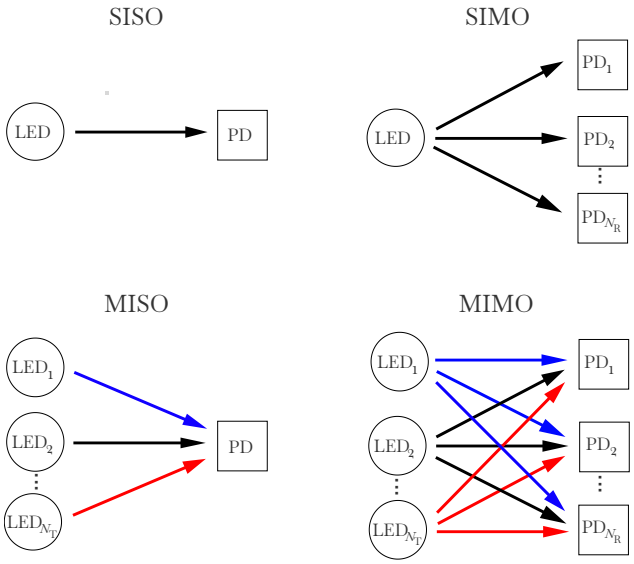

Fig. 11. Illustration of the four general input-output architectures from single-input single-output (SISO) to multiple-input multiple-output (MIMO). (N_{T} and N_{R} are the number of elements at the transmitter and receiver side, respectively).

domain is proportional to κ and proportional to the squared received power in the optical domain [25], [69]. Therefore, the larger κ, the better is the power efficiency of the optical modulation scheme given the same received power in the optical domain. This result is remarkable, because in many publications a reduction of the peak-to-average power ratio is recommended for hardware reasons (analog-to-digital and digital-to-analog conversion, power amplification), notably in the context of multi-carrier modulation schemes. Subsequently, these hardware problems are reduced by a superposition of waveforms with just two amplitude levels.

In [23], [25], more than 80 different intensity modulation methods based on a single light source and a single PD are reported, with about 20 more array-based methods (so-called MIMO techniques). Since a survey is not targeted here, in the next subsections a common framework is presented instead.

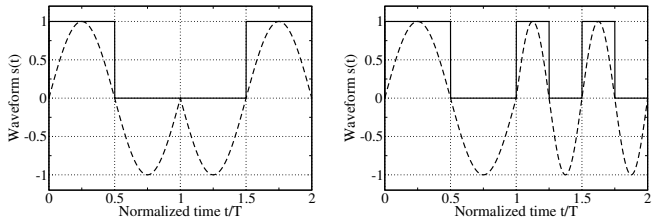

Fig. 12. Bi-phase PSK and FSK waveforms obtained by the concept of rectification (solid lines). The first symbol corresponds to data bit "0", the second symbol to data bit "1". Here, the peak power is constrained. Alternatively, the average transmit power could be constrained.

C. SISO Modulation Schemes

Let us start with the simplest setup comprising a single light source and a single photodetector, called single-input single-out (SISO) modulation schemes (Fig. 11). Scenarios with multiple light sources and/or photodetectors will be reported in Section III-D. SISO modulation schemes can be classified as single-carrier and multicarrier modulation schemes.

Single-Carrier Modulation Schemes with Two Amplitude Levels: Semiconductor LEDs can not be switched "on" and "off" arbitrarily fast. For example, white LEDs have a bandwidth of about 2 MHz, whereas red/green/blue (RGB) LEDs have a bandwidth of about 20 MHz. Modulation schemes with two amplitude levels, so-called bi-phase modulation schemes, are hardware-friendly for several reasons: (i) hard-switching is simpler than amplitude modulation, (ii) switching losses are small for modern semiconductor switches, therefore high-power solutions are feasible, (iii) no digital-to-analog converter (DAC) is necessary at the transmitter side, and (iv) threshold detection may replace an analog-to-digital converter (ADC) at the receiver side in low-cost implementations. On-off keying (OOK), pulse-position modulation (PPM), and pulse width modulation (PWM) are among the most popular bi-phase modulation schemes. In order to provide a common framework, we propose the concept of "rectification". We refer to rectification as two-level quantization. Given a classical binary modulation scheme like phase-shift keying (PSK) or frequency-shift keying (FSK), the corresponding rectified version can be obtained by employing a Schmitt trigger, whose threshold level is adjusted to the mean value of the analog waveform. That way, waveforms with two amplitude levels are obtained (Fig. 12). It is interesting to note that binary PPM is identical with rectified PSK if one period corresponds to one symbol duration T. In the case of rectified PSK, however, multiple symbol periods may be allocated to one symbol duration.

These bi-phase waveforms can easily be modified by introducing a variable duty cycle. The duty cycle is defined as "on" time divided by "on plus off" time. Increasing/decreasing of the threshold of the Schmitt trigger reduces/increases the duty cycle. For example, given a sine function, a threshold of $\pm\sin(\pi/4)$ yields a duty cycle of 25 % and 75 %, respectively. A selection of resulting waveforms, called VPSK, VFSK, VOOK and VPPM (variable PSK/FSK/OOK/PPM) are depicted in Fig. 13. In indoor communications, VPPM is used for dimming, but VPSK, VFSK, and VOOK seem to be novel. In UOWC, bi-phase modulation schemes with variable duty

This article has been accepted for publication in a future issue of this journal, but has not been fully edited. Content may change prior to final publication. Citation information: DOI 10.1109/COMST.2021.3111984, IEEE Communications Surveys & Tutorials

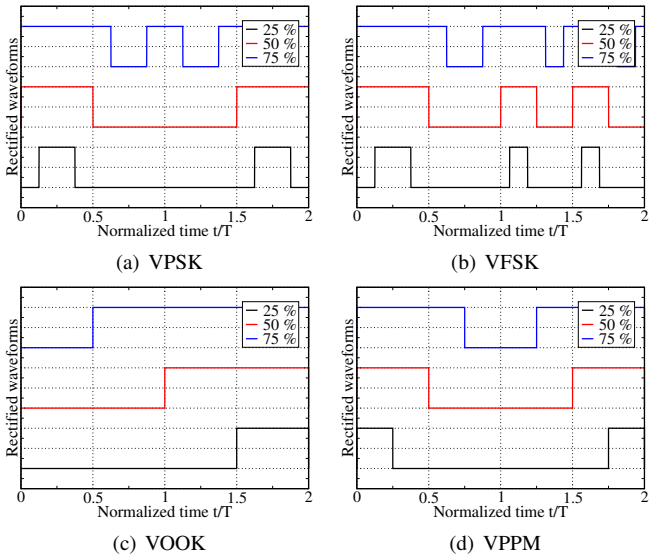

(a) VPSK (b) VFSK

(c) VOOK (d) VPPM

Fig. 13. Selection of bi-phase waveforms with varying duty cycle (in percent). The first symbol corresponds to data bit "0", the second symbol to data bit "1". Here, the peak power is constrained. Alternatively, the average transmit power could be constrained.

cycle are useful for power control – a fact which is frequently overlooked. This fact is important in light of the scarce power budget.

Multi-Level Single-Carrier Modulation Schemes: Multi-level modulation schemes like Q-ary PAM can often be decomposed into modulation schemes with two amplitude levels. Since a common framework is targeted, it is sufficient here to point out the possibility of a weighted superposition of two-level waveforms. For instance, 8-ary PAM with equidistant symbol spacing can be obtained by a superposition of three independent binary data streams, so-called layers, with amplitudes 1, 2, and 4, respectively. In Section III-D further details are reported in the MIMO context.

Multicarrier Modulation Schemes: One of the most popular multicarrier schemes is orthogonal frequency-division multiplexing (OFDM). In OFDM, N complex-valued sinusoids with frequency n/T_u $(0 \leq n \leq N-1)$ and length $T_u = N\,T$ are superimposed, the so-called subcarrier signals. Correspondingly, all subcarrier pulses have a sinc-type Fourier spectrum that is equally spaced by $1/T_u$ in the frequency domain, hence the subcarriers are orthogonal. Each subcarrier is usually modulated by a different complex-valued (e.g., QAM) data symbol. In other words, N independent data symbols are processed and transmitted simultaneously. The symbol rate is $1/T$. OFDM signals can be realized by the inverse discrete Fourier transform (IDFT). The data symbols can be recovered at the receiver side by the corresponding discrete Fourier transform (DFT). Essentially, the DFT acts like a bank of matched filters, each of which is matched to the corresponding subcarrier pulse, followed by rate $1/T_u$ sampling. As long as the orthogonality is maintained, data recovery is not degraded by the linear superposition. Channel dispersions (caused by multipath propagation and/or a finite-bandwidth light source) can be compensated by extending the useful symbol duration T_u by a cyclic prefix, also called cyclic extension. In simple words, the symbol duration is made longer, but the detection interval is kept to be T_u. Thus, intersymbol interference is completely avoided as long as the cyclic prefix is not shorter than the length of the delay spread.

In wideband communication systems, multicarrier modulation schemes and particularly OFDM are popular for several reasons: (a) In conjunction with a cyclic prefix, channel dispersions can be mitigated by a single-tap equalizer; (b) In conjunction with adaptive power allocation based on the water-filling theorem plus adaptive bit allocation, the power-bandwidth resources can be exploited efficiently; (c) An adaptation to different channel conditions is simple; (d) An extension to multiple access is straightforward by allocating resource blocks to different users. Besides these advantages, nonlinear distortions are a bottleneck as this kind of distortion destroys the orthogonality. In the context under investigation, the nonlinear large-signal behavior of LEDs is cumbersome. Vice versa, optical multicarrier systems benefit from a large average-power-to-squared-mean ratio κ [25], [69].

Regarding equalization, multipath is not critical in underwater communications since NLOS paths are attenuated significantly more than the LOS path. In OWC and UOWC, however, two key issues need to be considered, which have a negative impact on the power/bandwidth efficiency. One of these issues is that OFDM signals are complex-valued, even for real-valued data symbols. Hence, classical OFDM is not suitable for intensity modulation.

A real-valued transmit signal can be obtained by exploiting the fact that the superposition of two complex-valued vectors with reverse phase yields a real-valued vector. Recall that in OFDM each subcarrier signal can be represented by a complex-valued sinusoid, i.e., a phasor. The trick now is to superimpose a phasor onto a phasor with opposite phase. Towards this goal, only the $N/2$ lower subcarriers are modulated with random data. The $N/2$ upper subcarriers are modulated with exactly the same data, but opposite phase. This trick is called Hermitian symmetry and illustrated in Fig. 14. Hermitian symmetry guarantees a real-valued waveform for all possible combinations of QAM data symbols. However, the spectral efficiency is degraded by a factor of two compared to QAM-OFDM, because the upper subcarriers do not carry any new information. Additionally, the direct current (DC) subcarrier and the middle subcarrier are left empty, since otherwise the bias would be data-dependent. The corresponding waveform is dubbed discrete multitone transmission (DMT).

DMT signals are bipolar and therefore can also take negative values. This is the second key issue to be solved. Starting-off from DMT, this problem can be avoided by a positive bias term and by clipping the remaining negative values, dubbed DC-offset OFDM (DCO-OFDM) [70], [71]. The bias term has a negative impact on the power efficiency of the communication unit, because it does not contribute to data detection. The clipping also degrades the power efficiency because orthogonality gets lost ("clipping loss"). The larger the bias, the rarer are negative samples. For these reasons, the bias should be optimized. The bias can be added in the digital domain or by a bias-T, respectively.

Again starting-off from DMT, compared to DCO-OFDM a

This article has been accepted for publication in a future issue of this journal, but has not been fully edited. Content may change prior to final publication. Citation information: DOI 10.1109/COMST.2021.3111984, IEEE Communications Surveys & Tutorials

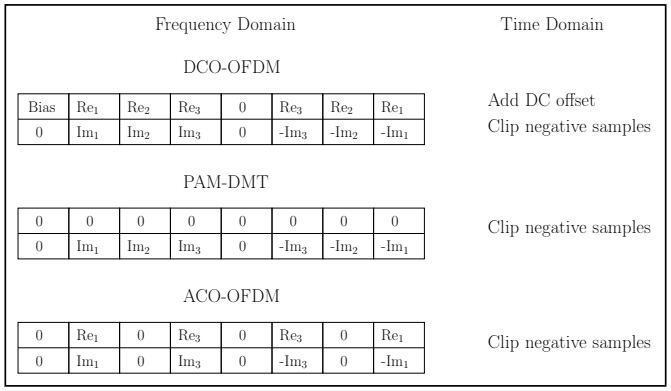

Fig. 14. Comparison of DCO-OFDM, PAM-DMT, and ACO-OFDM ($N = 8$ subcarriers). Simplified modification of [25].

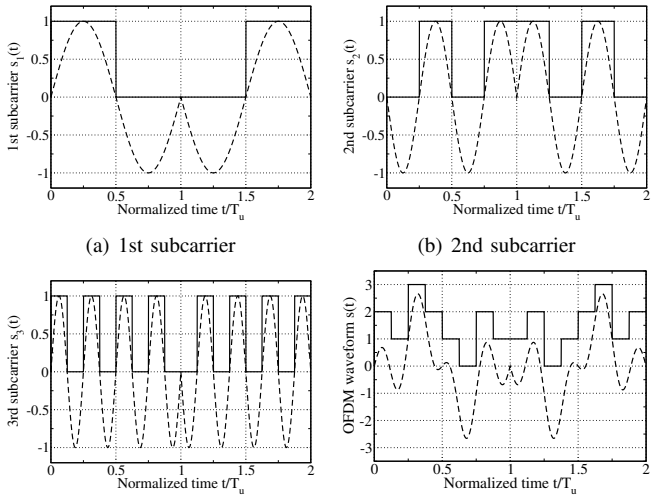

Fig. 15. Design of multicarrier modulation schemes based on the concept of rectification. ($N = 3$ orthogonal subcarriers for illustrative purposes. The ratios between all subcarrier frequencies are multiples of two. The data sequence is 01, 10, 01.)

more elegant and efficient solution is obtained by using only imaginary-valued PAM data symbols in the frequency domain. It can be shown that then the time-domain waveform consists of modulated sine functions rather than modulated complex-valued sinusoids. Since the sine function is real-valued and odd, positive and negative signal components occur pairwise. Negative signal components are redundant and hence can be clipped without performance loss. This technique is called pulse amplitude modulation based DMT (PAM-DMT) [72]. As opposed to DCO-OFDM, clipping happens for half of the samples.

Another elegant solution based on Hermitian symmetry is to leave all even subcarriers (in the frequency domain) empty. Consequently, the negative part of the transmit signal (in the time domain) is redundant, and hence can be clipped without loss of information even in the absence of a bias term. This version is called asymmetrically clipped optical OFDM (ACO-OFDM) [71], [73]. Odd subcarriers are loaded with complex-valued data. Compared to QAM-OFDM, ACO-OFDM suffers from a 3 dB power loss (because of clipping) and a factor of four in spectral efficiency. Fig. 14 provides a comparison of DCO-OFDM, PAM-DMT, and ACO-OFDM.

A novel and unpublished method is to realize OFDM, DMT, DCO-OFDM, PAM-DMT, and ACO-OFDM (and related multicarrier versions) by means of rectification. Towards this goal, we propose to replace sine/cosine functions by the corresponding rectified waveform. Fig. 15 illustrates this novel multicarrier design. Note that orthogonality is maintained if the ratios between all subcarrier frequencies are multiples of two, although each subcarrier has just two amplitude levels in the time domain. Further notice that the superimposed waveform is not just a quantized version of the analog waveform as proposed in [74], [75]. Each subcarrier can drive an individual light source in order to avoid the implementation problems related to OFDM/DMT/DCO-OFDM/PAM-DMT/ACO-OFDM. The light sources are either part of the same luminary, or they are spatially distributed. In the former case, either a single power supply can be used, or each light source can be driven by its own power supply in order to boost the luminance. Vice versa, dimmable MC communication is possible by adaptively changing the duty cycle as proposed in Section III-C, at the cost of loss of orthogonality, however.

D. MIMO Modulation Schemes

Optical MIMO schemes are characterized by $N_{\mathrm{T}} > 1$ transmit elements and $N_{\mathrm{R}} > 1$ receive elements. In mobile UOWC applications, the transmit elements are LEDs with the same or with different colors. MIMO topologies are important for several reasons:

- A spatial multiplexing gain is achievable if different data streams are transmitted via the transmit elements. The channel capacity is proportional to $\min(N_{\mathrm{T}}, N_{\mathrm{R}})$. Spatial multiplexing boosts the data rate and peak throughput and thus increases the spectral efficiency.
- A spatial diversity gain is resolvable if the same information is transmitted via several Tx apertures and/or received via several Rx apertures. Spatial diversity reduces the error rate and outage and thus improves the power efficiency.
- LEDs and PDs are either co-located or spatially distributed. Multiuser communication is a special case.
- Besides single-user and multiuser communications, MIMO processing is also useful for localization.

Recall that the amplitude variations of the transmit signal should be as large as possible in order to maximize the received power in the electrical domain given a certain received power in the optical domain. There are several possibilities to realize and to implement modulation schemes with large signal variations. For instance, OFDM and its DMT variants can be used, because multicarrier modulation schemes inherently have large amplitude fluctuations caused by the linear superposition of statistically independent subcarrier signals. These continuous-valued modulation schemes can be processed using analog circuit technology, as shown in the top part in Fig. 16. A simple yet efficient alternative is the spatial summing architecture [74]–[76], plotted in the bottom part. Inherently, the

This article has been accepted for publication in a future issue of this journal, but has not been fully edited. Content may change prior to final publication. Citation information: DOI 10.1109/COMST.2021.3111984, IEEE Communications Surveys & Tutorials

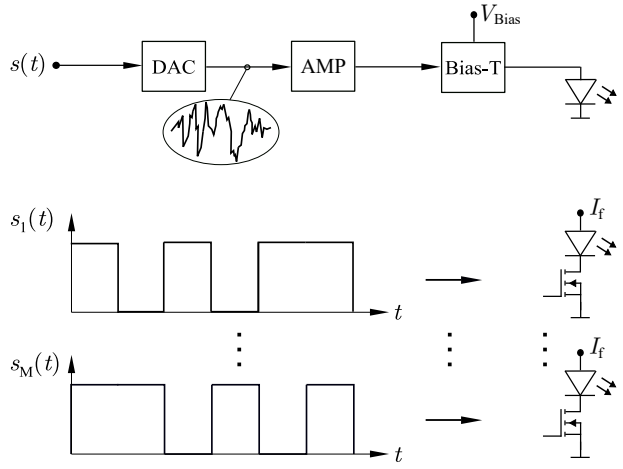

Fig. 16. Analog hardware (top) versus spatial summing architecture (bottom). In software-defined radio modems, the input signals are delivered by a digital signal processor, a microcontroller, a field-programmable gate array, or a related hardware platform. In the spatial summing architecture, digital output pins are sufficient.

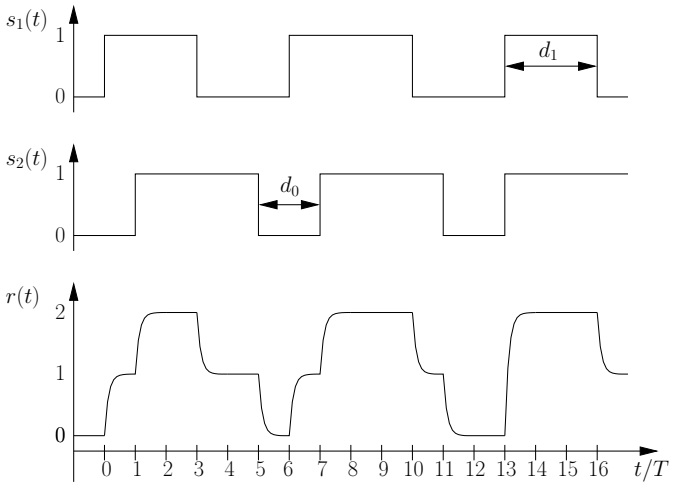

Fig. 17. Example for $(d_0|d_1)^{N_{\text{T}}} = (2|3)^2$ CSIM given $N_{\text{T}} = 2$ light sources. Both square waveforms $s_1(t)$, $s_2(t)$ fulfill the minimum "on" time constraint $d_1 = 3$ and "off" time constraint $d_0 = 2$. The superimposed received signal $r(t)$ is shown in the bottom part. Figure redrawn from [76].

spatial summing architecture is a spatial modulation scheme. It is a multiple-input single-output (MISO) technique if applied with a single photodetector, or a multiple-input multiple-output (MIMO) technique in conjunction with several receive apertures. But even SISO modulation schemes can be realized by the summing architecture as already indicated in Section III-C.

Superposition modulation (SM) is a family of pulsed modulation methods based on binary-controlled LED arrays. Each LED is either "on" or "off". Information is encoded in the sum of the intensities. Summation takes place at the photodetector(s). Advantages of superimposed square wave signals include the following items: (i) The spatial summing architecture is inherently rate adaptive; (ii) The average-power-to-squared-mean ratio κ is large; (iii) There are no losses due to nonlinearities; (iv) The spatial summing architecture is suitable for multiuser communication; (v) The circuit technology is simple and inexpensive; (vi) No DAC is necessary at the transmitter side.

A special case is constrained superposition intensity modulation (CSIM) [76]. "On"/"off" times can be adapted to the rise/fall times of the given LED. Each LED must be "on" ("off") for at least d_1 (d_0) clock cycles (see Fig. 17). The degrees of freedom can be increased by time-shifting the individual signals, which can possibly be exploited for increasing the data rate. The transmit signal is quasi analog for a sufficient number of layers, although each layer is binary. By means of sophisticated coding, in [76] the number of switching events have be minimized, i.e., switching loss has been minimized. CSIM is well suitable for OWC and particularly UOWC because of items (i)-(vi) and the following additional advantages: (vii) CSIM is characterized by the lowest possible switching loss; (viii) It can be matched to the rise/fall as well as the cool-down times of the light sources; (ix) Time-shifting the layers increases the degrees of freedom for signal design. A practical application of CSIM is shown in Section VI-C.

E. MISO versus SIMO Architectures

According to (3), in the electrical domain the received power in a SISO setup is proportional to the transmit power and the effective photosensitive area of the photodetector. Correspondingly, the SNR can be boosted by increasing both parameters. Traditionally, several LEDs are implemented in an optical Tx frontend. All LEDs usually operate in parallel, known as optical repetition coding or spatial repetition coding. This option is a MISO architecture (see Fig. 11). Alternatively, multiple photodetectors could be implemented in an optical Rx frontend. This option is called SIMO architecture subsequently. The question is: which of these optical frontend architectures is most efficient?

Let N_T denote the number of LEDs and N_R the number of photodetectors. All LEDs and photodetectors, respectively, are assumed to come from the same series. Interestingly, for $N_{\text{T}} = N_{\text{R}}$ the SNR is exactly the same for the same noise level, as $(N_{\text{T}}P_{\text{T}})A_{\text{R}} = P_{\text{T}}(N_{\text{R}}A_{\text{R}})$. However, the LED driver is the most power-hungry unit in a UOWC modem. Roughly speaking, the total power consumption is about proportional to N_T, whereas the power consumption of the TIA unit is much less (even in the worst case where N_R TIAs would operate in parallel). This statement strongly promotes the SIMO architecture. Still, a closer look at the noise power is necessary. Recall from Section II-E that two noise sources are dominant at the receiver side: shot noise and thermal noise. In the following, the contributions of shot noise and thermal noise are investigated for both the MISO and the SIMO architecture. The SISO setup is taken as a reference in order to avoid formulas.

Let us start with the shot noise. The shot noise is proportional to the received power at the photodetector. In shallow water, ambient light is dominant whereas in deep water the desired light source is prevailing. Let us analyse the deep water scenario without ambient light first. In the $N_{\text{T}} \times 1$ MISO scenario, the shot noise power is N_{T} times larger than

This article has been accepted for publication in a future issue of this journal, but has not been fully edited. Content may change prior to final publication. Citation information: DOI 10.1109/COMST.2021.3111984, IEEE Communications Surveys & Tutorials

in the SISO reference setup if all light sources operate in parallel. Similarly, in the $1\times N_{\mathrm{R}}$ SIMO scenario, the shot noise power is N_{R} times larger than in the SISO reference setup if the photodetectors are operated in parallel. For $N_{\mathrm{T}} = N_{\mathrm{R}}$, MISO and SIMO topologies are equally sensitive regarding the shot noise in the absence of ambient light. In the shallow water scenario with strong ambient light, the SISO and MISO architectures are equally affected by shot noise, whereas in the SIMO architecture the shot noise power is N_{R} times stronger. This statement is in favor of the MISO architecture. It's a motivation for ambient light suppression, studied in Section V.

The thermal noise is mainly caused by the TIA. For this reason, in the SIMO architecture only a single TIA is assumed and all N_{R} photodetectors are connected in parallel (although that TIA would have to deal with a much larger junction capacitance of all those PDs). In a good approximation, the thermal noise power is inversely proportional to the feedback resistance R_{f}. First, we assume that R_{f} is fixed for all topologies. Then, the thermal noise power is the same for the three architectures under investigation, but the received power is larger for the MISO and SIMO architectures. A constant TIA output voltage would be more fair. This can be obtained by dividing R_{f} by N_{T} and N_{R}, respectively. Then, the thermal noise power would increase by N_{T} in the MISO case and by N_{R} in the SIMO case. For $N_{\mathrm{T}} = N_{\mathrm{R}}$, MISO and SIMO topologies are equally sensitive regarding the thermal noise.

In summary, the SIMO architecture outperforms the MISO architecture in most scenarios, although the latter optical front-end design is more popular.

F. Cognitive Channel Adaptation

A cognitive system can not only monitor its own performance, but also environmental parameters. The system is able to recognize changes in the environment and to react on them. Cognitive channel adaptation is an important recipe for power savings and spectral optimizations. Subsequently, three different forms of cognitive intelligence are discussed in the context of UOWC suitable for underwater swarm robotics: power allocation and adaptive bit loading, reliability-based channel adaptation, and backscattering-based channel adaptation.

Power allocation and adaptive bit loading has already briefly been mentioned in conjunction with multicarrier modulation. Given subcarrier-wise channel estimates, in a first step power allocation can be performed by means of the waterfilling theorem. Accordingly, the SNR is different for each subcarrier. For this reason, in a second step for each subcarrier the most suitable modulation scheme can be selected, referred to as adaptive bit loading. Power allocation and adaptive bit loading are frequently based on training symbols that are spread in time and frequency domain as explored in [77].

Reliability-based channel adaptation is an alternative solution to monitor the impact of the environment on the quality of data transmission. The main point is to apply detection/decoding with reliability information, also called soft-output detection/decoding [78]. In soft-output decoding, the classical hard-output decisions ("0", "1") are augmented by bit-wise reliability values. These reliability values can be processed so that reliability information is even available for data packets [79], [80], without resorting to the overhead caused by training symbols. Based on the reliability information, the data rate can be increased/decreased in subsequent frames. In time-division duplexing (see Section IV-A), not even a feedback channel is necessary.

Another possibility for monitoring environmental parameters is to estimate optical backscattering power. To this end, an optical duplex communication system with hemispherical transceivers (cf. Section VI-A) is required, where transmitting LEDs and receiving PDs are co-located. With proper alignment, this causes predefined sectors of the LED transducer to overlap with the FOV of specific PDs [81], [82]. If the Tx sector then radiates into the water column, some of the optical power is backscattered by organic particles towards the transceiver, where it is measured by the PD. The reason why this setup is suitable for estimating the water quality, is that the amount of the scattered and thus also backscattered light depends on the turbidity of the water (see Fig. 2 and Fig. 3). The more turbid the water, the more particles are dissolved in it. Accordingly, a PD will measure a higher backscattering power in turbid water than in clear water. If the optical backscattering power and the precise orientation of predefined LEDs and PDs are known, the intersection of both LED FOV and PD FOV and thus the VSF can be determined [46], [83]. The latter describes the angular distribution of scattered light and is directly linked to the scattering coefficient b and the backscattering coefficient b_{b}. A cognitive system, which is monitoring these parameters can estimate the overall underwater attenuation coefficient K_{sys} and thus adaptively adjust the communication spectrum by switching between appropriate LED colors. As can be seen from Fig. 2 to Fig. 4, this will optimize the communication range because the wavelength experiencing the lowest attenuation varies with water quality.

G. Channel Coding

As noticed several times, power efficiency is of primary concern in the application under investigation. Approaching this goal, channel coding is an important recipe. Channel coding can be classified as forward error correction coding (FEC), automatic repeat request (ARQ) schemes, and line coding.

FEC is used for error detection and correction. At the transmitter side, redundancy is added in form of symbol repetitions and/or parity symbols. This redundancy is exploited at the receiver side in order to reduce the error rate. Due to the redundancy, there is a trade-off between power efficiency (necessary SNR to fulfill a given quality constraint) and spectral efficiency (number of bits per symbol per Hertz). In FEC schemes, there is no feedback from the receiver side to the transmitter side. Among the main families are block codes and convolutional codes, respectively [84]–[86]. Performance results for FEC-encoded UOWC systems are reported for instance in [39], [40].

In the case of block codes, both encoding and decoding is performed blockwise. Given k information symbols of

This article has been accepted for publication in a future issue of this journal, but has not been fully edited. Content may change prior to final publication. Citation information: DOI 10.1109/COMST.2021.3111984, IEEE Communications Surveys & Tutorials

cardinality q, $n-k$ redundant symbols are added to obtain a code word. Each info code word of length k is assigned to exactly one code word of length n. The code rate is $k/n < 1$ and hence the bandwidth expansion is $n/k > 1$. Since only q^k possible code words exist, error detection and error correction is possible. Among the most popular block codes are Reed Solomon (RS) codes, low-density parity check (LDPC) codes, and polar codes. RS codes ($\sim$1960) are frequently used for the correction of burst errors [87]. Algebraic decoding is typically performed given hard decisions by the demodulator. Long irregular LDPC codes ($\sim$1995) are able to operate close to the channel capacity [88]. LDPC codes are usually iteratively decoded employing real-valued decoder input values. Polar codes have only recently been discovered ($\sim$2010), they are provable capacity achieving [89].

In contrast to block codes, convolutional codes are able to perform continuous encoding and decoding [84], [85]. At the transmitter side, the data sequence is processed by a shift register. At the receiver side, graph-based decoders are implemented, typically taking care of real-valued decoder input values.

Besides pure block codes and convolutional codes, since the 1990s concatenated block or convolutional codes have extensively been studied, including Turbo codes [90]. In turbo codes, two or more convolutional codes are concatenated in parallel. At the receiver side, reliability information is passed between the corresponding constituent decoders, similar to message passing in LDPC codes. Turbo codes operate reasonably close to the channel capacity.

Contrary to FEC schemes, in ARQ schemes a feedback channel between the decoder and the encoder is established [85]. Classically, error detection is performed based on block coding. If the number of detected errors exceeds the number of correctable errors, retransmission will be requested via the feedback channel. Either the entire code word will be retransmitted, or just additional redundancy. Therefore, ARQ always causes a certain delay, depending on the number of retransmissions. The combination of ARQ (based on an error detection code) and an error correction code is called hybrid ARQ (HARQ). An interesting solution is to avoid the error detection code by exploiting receiver-side reliability information in order to declare whether a retransmission is necessary or not [80]. Another recent innovation are fountain codes [85], [91]. Given a fixed info word length k, incremental redundancy is added until decoding is possible. For this reason, fountain codes are rateless.

Efficient error recovery in underwater sensor networks is also possible by means of network coding [92], [93]. In network coding, data packets are efficiently routed via a communication network, where intermediate nodes serve as relays. Unlike classical routing, which does not change the contents of the messages (like in postal mail), in network coding the nodes combine several input packets into one or several output packets by means of a modulo addition or linear combining. Network coding does not simply concatenate data packets. The pros of network coding include robustness and/or throughput enhancement and/or data security, at the expense of computational complexity.

The purpose of line coding is spectral shaping [94]. Long runs of 0s or 1s cause a bias, i.e., a DC component. Among the undesired effects in OWC are flicker, overheating of the light source, and synchronization problems. These issues can be avoided with line codes by controlling the runlength. In the simplest case, bit "0" is replaced by "01", whereas bit "1" is replaced by "10". Of course, more sophisticated line codes with higher efficiency exist. An alternative to line coding is scrambling. In scrambling, the runlength is controlled by XORing the bit sequence with a pseudo-random binary sequence. That way, redundancy is avoided completely, but runlength control is performed only statistically.

In order to improve the spectral efficiency, it is advisable to combine channel coding with the modulation scheme. In bit-interleaved coded modulation (BICM), the channel encoder is separated from the modulator by a bit-wise interleaver [95]. Consequently, a serial concatenated coding scheme arises. At the receiver side, iterative detection can be performed by passing reliability information between the demodulator and the decoder in order to improve the error performance. An alternative to BICM is superposition modulation/coding (SM), where coded binary data sequences are linearly superimposed [96]. Regarding an adaptation to variable channel conditions, in the case of BICM typically the cardinality of the modulation alphabet is changed, whereas in the case of SM the number of binary data sequences is adjusted.

In optical communications, a target bit error rate threshold is frequently declared for the uncoded case, for example 10^{-3}. Transmission is declared to be reliable, if the uncoded performance is less than this threshold, since then the residual error rate after channel decoding can assumed to be arbitrarily small. When employing decoding with reliability information, called soft-output decoding, the average bit error rate can be estimated for each individual data packet without resorting to training data. In soft-output decoding, the decoder delivers a reliability value together with the hard decision for each individual information bit.

H. Equalization

In the field of underwater swarm communication, high-rate data transmission between the swarm elements is targeted. With increasing data rate, however, the symbol duration reduces. In the presence of channel dispersions, intersymbol interference (ISI) is likely. ISI has a negative impact on the bit error performance, i.e., transmission gets unreliable. Hence, either data packets are lost or the number of retransmissions become excessive. ISI can be compensated by means of equalization [97].

Recall that in UOWC, channel dispersions are due to the finite bandwidth of LEDs, pulse shaping and receive filtering, as well as multipath propagation. The spectral characteristic of LEDs can be approximated by a first-order lowpass filter. With sophisticated driver circuits, the rise and falls times can be reduced and hence the length of the impulse response can be shortened. The influence of pulse shaping and receive filtering on the impulse response is deterministic as well and can be controlled by proper hardware and software design [25].

This article has been accepted for publication in a future issue of this journal, but has not been fully edited. Content may change prior to final publication. Citation information: DOI 10.1109/COMST.2021.3111984, IEEE Communications Surveys & Tutorials

Multipath propagation is fairly moderate since the LOS path typically is dominant in UOWC. If the LOS path is blocked, transmission is likely to fail. For these reasons, in UOWC usually no sophisticated equalizer is necessary. Nevertheless, for data rates in the Mbps range, ISI compensation is recommendable.

In single-carrier transmission schemes, a guard interval is among the simplest solutions. This equalization strategy is particularly suitable for waveforms with two amplitude levels. Data symbols either start with an off-period, or each data symbol is made somewhat longer. At the receiver side, not the entire symbol duration is exploited for data detection, but only the second part of a data symbol since the first part is affected by the second part of the previous symbol. When the length of the guard interval is not shorter than the length of the impulse response of the channel, ISI is compensated completely.

A special case where a guard interval is exploited inherently is return-to-zero on-off keying (RZ-OOK). As opposed to non-return-to-zero on-off keying (NRZ-OOK) where the duration of the on-period corresponds to the symbol duration, in RZ-OOK the on-period is shorter than the symbol duration. If the on-period is sufficiently small, ISI is avoided completely.

In multicarrier transmission schemes, a cyclic prefix is a popular method in order to compensate ISI, see Section III-C. A cyclic prefix is related to the concept of the guard interval: the symbol duration is extended cyclically, i.e., made somewhat longer. At the receiver side, the cyclic prefix will be removed, and therefore only the second part of each symbol is exploited for data detection. This technique is dubbed one-tap equalization.

In situations with deterministic dispersions, equalization can also be compensated at the transmitter side. This concept is called precoding. Precoding avoids noise enhancement and noise shaping, which are the main bottlenecks of conventional equalizers [97]. Tomlinson-Harashima precoding is an example frequently discussed in the areas of fiber optics and terrestrial wireless radio. In OWC and UOWC, precoding is still an emerging topic.

Last but not least, it should be emphasized that equalization belongs to the class of detection schemes. As already mentioned in the previous subsection, decoding/detection with reliability information (i.e., soft-input soft-output processing) is an important recipe for power-limited communication schemes. This aspect is commonly overlooked in the area of UOWC.

IV. Data Link Layer Aspects and Hybrid Transmission Schemes

A. Duplexing Strategies

In bidirectional (i.e., duplex) communication, both links (called forward/return link or uplink/downlink) need to be separated. Frequency-division duplexing (FDD) and time-division duplexing (TDD) are most common.

In FDD, paired frequencies are reserved: one for the forward link, the other one for the return link. The optical analogon is wavelength-division duplexing (WDD). For example, blue and green can be used for the forward and return link, respectively. At the receiver side, color filtering is necessary.

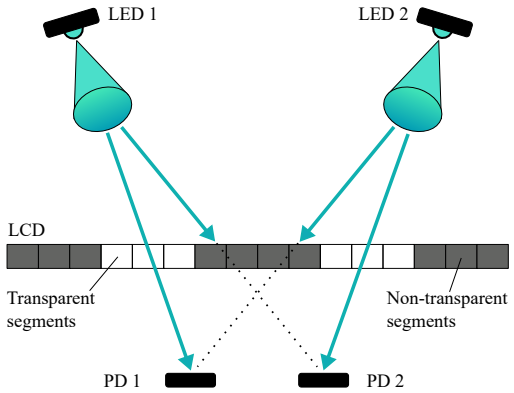

Fig. 18. Illustration of LCD-based small scale SDMA. To separate LED 1 from LED 2, those pixels are switched transparent that are in the direct path between desired LED and corresponding PD. Figure based on [98].

In TDD, separated time slots are allocated for both links. This duplexing strategy is applicable to UOWC as well. There are at least two advantages of TDD: the peak wavelength can be optimized with respect to the narrow optical window, and varying traffic can easily be adjusted by varying time slots. Unlike WDD/FDD, in TDD the physical channel conditions are identical for the forward and return link, which simplifies environmental monitoring.

B. Multiuser Access

Multiple access schemes allow different users to share the same resources like time, frequency, and space [41]. Optical communication in AUV swarms requires the employment of smart multiuser strategies. Otherwise, in the worst case, crosstalk between signals transmitted from different communication nodes makes a receiver-side separation difficult.

A straightforward approach is to use the time-division multiple access (TDMA) strategy, where each node is assigned a specific time slot for communication. This avoids overlapping with signals from other users. If time synchronization between all nodes in an AUV swarm is possible, time slots can be assigned multiple times, similar to frequencies in a cellular network. This is possible because identical time slots will be assigned exclusively to nodes that are sufficiently separated in space and because the FOV of LEDs is limited. That way, overlapping and thus interference can be avoided.

Wavelength-division multiple access (WDMA) is another strategy that can be employed for multiuser communication in an AUV swarm. Here, different nodes are assigned different wavelengths, i.e. LED colors, that are used for communication, similar to frequency-division multiple access (FDMA) and orthogonal frequency-division multiple access (OFDMA). However, for this strategy to be applicable, certain requirements have to be fulfilled. First, the wavelengths have to be sufficiently far apart. This will ensure that the corresponding spectra do not overlap. In UOWC, however, only blue, cyan, green and sometimes yellow are suitable, see Section II. Second, optical bandpass filters that are tailored to the used LED colors have to be employed to minimize interference.

In space-division multiple access (SDMA) users are separated in the spatial domain. In UOWC, this can be achieved

This article has been accepted for publication in a future issue of this journal, but has not been fully edited. Content may change prior to final publication. Citation information: DOI 10.1109/COMST.2021.3111984, IEEE Communications Surveys & Tutorials

by spot beams. Spatial multiplexing, originally proposed for a single user [99], can be slightly modified to become a spatial multiple access scheme as well.

A special version of space-division multiple access is small-scale SDMA. While in traditional SDMA there are no restrictions regarding the spatial separation of transmitters/receivers, "small scale" refers to multiple receivers being co-located in one communication node. To achieve user separation, an LCD with high contrast (which we know from automatic welding filters, for instance) can be employed and placed in front of the PD array [98], [100]. The pixels of the LCD are individually switchable to transparent or non-transparent mode. Assume an exemplary swarm communication scenario between two transmitting nodes and one receiving node with two co-located PDs, as illustrated in Fig. 18. In this case, both users can be separated at the receiver side by switching most areas of the LCD to the non-transparent mode, leaving only two translucent areas that are in the direct path between the desired transmitter and the corresponding PD. In other words, interfering light sources are blocked and the communication channels are decorrelated.

Another option for multiple access in AUV swarms is optical code-division multiple access (OCDMA) [101]. In OCDMA, each user is assigned a specific spreading sequence – similar to the ID number in passports. The spreading sequences are data-independent. The cross-correlations between the spreading sequences should be as small as possible. If all sequences are mutually orthogonal, cross-talk is zero. In combination with OOK, given an information bit "1" the user-specific spreading sequence is being transmitted. Vice versa, the transmitter is silent for a symbol period if the information bit is "0". OCDMA either operates in synchronous mode ("synchronous OCDMA") or asynchronously ("asynchronous OCDMA"). The latter option is easier to implement in swarms, but crosstalk is not avoidable without time synchronization.

A special case of OCDMA is interleave-division multiple access (IDMA). In IDMA [102], the same spreading sequence is used for all users. This spreading sequence, however, is permuted by pseudo-random interleavers. Each user is assigned a user-specific interleaver.

Non-orthogonal OCDMA and IDMA belong to the family of non-orthogonal multiple access (NOMA) schemes [103]. NOMA schemes are capable to provide high connectivity. It can be shown both for multiple access channels (uplink) and broadcast channels (downlink) that NOMA schemes are able to outperform orthogonal multiple access techniques like WDMA/FDMA/OFDMA, TDMA, and SDMA at the expense of an increased receiver complexity, because the receiver must be able to separate all data sequences.

C. Multihop Transmission and Optical Relaying

For the successful deployment of AUV swarms, a robust, high-rate communication link is necessary at all times. The reason is that for coordination, mission planning and management, the positions of all nodes must always be known and it must always be possible to exchange critical mission data. On top, beamforming is necessary to provide a sufficient SNR. However, in the underwater environment, light is subject to wavelength-dependent absorption and scattering, which results in much stronger signal attenuation than in air. This significantly limits the underwater communication range. Furthermore, beam steering is not always perfect, which likely causes outage. One possibility to improve the communication range and reliability is to employ hybrid transmission schemes, where different communication technologies are used jointly (cf. Section IV-D).

Another possibility to extend the communication range is to use optical single-hop and multi-hop relaying [25], [41], [104], [105]. However, for this purpose, all swarm nodes, e.g. AUVs, ROVs and ground-based communication nodes, must be capable of performing relaying. In other words, a node must be able to receive an optical signal, process it and then retransmit it to the next node. For relaying of optical signals, two well known principles are particularly interesting: amplify and forward (AF) and decode and forward (DF) relaying. In the first design, the signal is received, amplified, and directly forwarded to the next node. The second principle requires more steps. Here, the signal is received, demodulated and decoded, and then encoded and modulated before retransmission. The advantage of AF, compared to DF, is that only a fraction of the processing steps are performed, which results in a lower latency and a simpler design. However, shot noise is amplified and a DC-bias results from sunlight. Methods for ambient light compensation include circuit design solutions, mechanical construction, and optical filtering techniques [25]. DF, on the other hand, outperforms AF in terms of SNR and BER, because the signal is demodulated and decoded at each node. This avoids noise enhancement at each stage if the distances between relays are sufficiently small. That way, a large Tx-Rx distance can be covered if many relays are available.

Assume an exemplary swarm communication scenario, shown in Fig. 1, between the communication node anchored to the ground and the two AUVs in the center of the picture. Furthermore assume that the Rx node (in this case the AUV near the water surface) is out of range of the Tx ground node. Operating in relaying mode, the Tx ground node transmits the signal to the neighboring relay AUV rather than directly to the receiver. The relay AUV then processes the received signal and retransmits it to the Rx AUV. Thus, even though Tx ground node and Rx AUV are effectively out of range, the optical signal can still be transmitted with the help of auxiliary nodes, which are capable of performing relaying. This process represents a single-hop relaying transmission, but it can be extended to a multi-hop transmission, if the signal is further retransmitted e.g. to the escorting ship.

D. Hybrid Transmission Schemes

Currently, there are four technologies available for wireless communication in the underwater environment [35], [40]–[45]. The most prominent and most frequently used technology employs acoustic waves, which enable communication links over distances of several tens of kilometers [7]–[9], [11]. However, as stated in Section I-B, the small communication bandwidth, the low and varying signal propagation speed,

This article has been accepted for publication in a future issue of this journal, but has not been fully edited. Content may change prior to final publication. Citation information: DOI 10.1109/COMST.2021.3111984, IEEE Communications Surveys & Tutorials

multipath propagation and Doppler spread limit their applicability in a real-time communication system for swarm robotics. Furthermore, acoustic transceivers usually are heavy, bulky, and power inefficient.

An alternative to acoustic modems is UOWC [25], [39]–[45]. Compared to acoustic waves, electromagnetic waves in the visible range benefit from a much higher propagation speed and much higher data rates. Furthermore, the invention of pressure-neutral resin casting of LEDs [106] now makes it possible to design very compact and lightweight optical transmitters and receivers that can be integrated streamlined into the AUV hull. However, UOWC is subject to wavelength-dependent absorption and scattering, which significantly limits the communication range.

Generally, also radio waves can be utilized for underwater wireless communication. However, the attenuation is severe. Decreasing the operating frequency would eventually reduce the attenuation, however, as indicated in Section I-B, this would lead to properties of the communication system that make radio frequency (RF) waves unsuitable for AUV swarm communication. For this reason, RF waves will not be considered in the following.

Finally, magnetic fields represent an alternative signal carrier for wireless underwater communication [34]–[36]. Compared to acoustic communication, MI communication benefits from small propagation delay and higher bandwidth. Compared to UOWC, the low sensitivity to water turbidity is an important advantage. Regarding data rates, in [33] theoretically achievable values in the Mbps range have been reported. However, it was also stated that an optimal operating frequency must be used to minimize path loss and that the effective bandwidth is severely limited in underwater transmission. Furthermore, replacing the receiver coil of the communication system by an AMR sensor (or equivalent) has proven to be advantageous, because this family of detectors offers a high bandwidth and is lightweight. That way, the weight can be reduced and both transmitter and receiver can be streamlined integrated into the AUV hull. The major disadvantage of MI communication is the generally strong attenuation, which, on top of that, is significantly increased in salty waters.

One possibility to compensate for the disadvantages of the above mentioned communication technologies, is to employ a hybrid communication strategy in which different technologies are combined adaptively and efficiently. Generally, there are three different operating modes that can be selected by a hybrid communication system. The first, depicted in Fig. 19, uses a microcontroller (μC) performing simultaneous transmission of the same data stream over all available communication channels. At the receiver side, spatial diversity is achieved by efficiently combining all received signals. If the noise processes are statistically independent, the optimum procedure is to add the log-likelihood ratios (LLR) of the data bits. But if the observations are correlated, the LLRs should be weighted before superposition [107]. However, a selection of this operation mode unfortunately maximizes the energy consumption since all subsystems are simultaneously active. Moreover, the data rate is limited by the subsystem with the smallest packet rate, because diversity combining can be

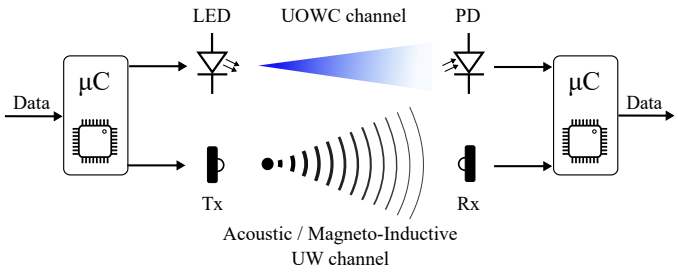

Fig. 19. Hybrid communication scheme achieving spatial diversity by simultaneously transmitting the same data over both communication channels.

completed only after the reception of data packets from all subsystems. Therefore, this operating mode should only be used as a backup solution for AUV swarm communication to increase the overall signal quality if the SNR and hence the channel capacity on all active communication channels is below a predefined threshold.

The second and third operating modes are shown in Fig. 20. Here, the microcontroller distributes the incoming data among all available subsystems depending on the prevailing channel conditions. The distribution process is characterized by the duty cycle $\alpha \in [0, 1]$. For simplicity and practical reasons, subsequently two subsystems are assumed.

If the microcontroller completely deactivates one technology, the system operates in hard-switching mode, thus transmitting the entire data stream via the wireless underwater channel, which remains active. In this case, α is either 0 or 1, i.e., $\alpha \in \{0, 1\}$. For example, if the entire data stream is to be transmitted exclusively over the UOWC channel, $\alpha = 0$ applies. Switching off a subsystem is advisable, if for example the distance between transmitting and receiving AUV exceeds the communication range, or the channel conditions are too poor for robust communication. On top of that, challenging mission circumstances may require the deactivation of certain technologies. If for instance a critical battery charge is imminent, the communication technology with the highest energy consumption should be switched off.

Operating the communication system in soft-switching mode represents the third alternative. Here, all technologies are used simultaneously and the data stream is efficiently distributed by the microcontroller to adapt the data rate to varying conditions of each communication channel and thus maximizing the overall performance. Unlike in the hard-switching case, α can now be in the range $0 < \alpha < 1$, thus excluding 0 or 1. Compared to the operating modes introduced so far, soft-switching thus offers the highest possible data rate, which, assuming optimal channel conditions, is calculated as the sum of the individual maximum data rates. Consequently, this operating mode should only be selected if sufficient power reserves and good channel conditions are available and if the distance between transmitting and receiving AUV is less than the smallest communication range.

Since the focus of this tutorial is on UOWC, only hybrid communication schemes that consider UOWC in combination with another technology are discussed in the following. In [108]–[112] it is proposed to complement high-bandwidth low-latency UOWC with robust underwater acoustical communi-

This article has been accepted for publication in a future issue of this journal, but has not been fully edited. Content may change prior to final publication. Citation information: DOI 10.1109/COMST.2021.3111984, IEEE Communications Surveys & Tutorials

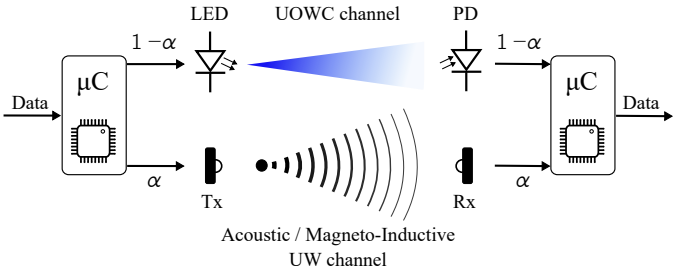

Fig. 20. Hybrid communication scheme enabling hard-switching mode ($\alpha \in \{0, 1\}$) and soft-switching mode ($0 < \alpha < 1$).

cation. In this context, two approaches for a hybrid optical-acoustic communication system are described. Considering the AUV swarm scenario, the first approach employs UOWC for high data rate, near-range communication, while acoustics serve as a backup technology for communication outside the optical range, or in turbid water. Another approach is to assign the communication technologies to different areas of application: while UOWC remains in use for inter-AUV communication, acoustic waves are employed, for example, for signalling events between sensor nodes or for exchanging mission objectives with the ship-based mission control. Considering the previously introduced operating modes, both approaches correspond to the hard-switching principle. Soft-switching is not advisable in this case, since the data rate would increase only marginally at the expense of significantly higher power consumption.

While hybrid optical-acoustic communication is already well studied [39], [40] and applied in several prototypes [108]–[110], [112], the combination of MI communication with UOWC is novel and largely unexplored. Nevertheless, considering the previously mentioned pros and cons, the combination seems very promising, as the technologies complement each other well. On the one hand, UOWC is well suited for clear water scenarios with good visibility and is little affected by salinity. However, robust communication becomes increasingly difficult as the turbidity of the water intensifies. MI, on the other hand, has a low sensitivity to water turbidity, but a strong signal attenuation in waters with high salinity. Considering the first of the previously introduced hybrid communication schemes, transmitting the same data over both the MI and the UOWC channel is advisable, if the turbidity as well as the salinity of the water is moderately high. For example, this is the case in the surf zone of the North Sea with a high average salinity of 3.4 % [113]. If either the salinity or the turbidity continues to increase until a predefined threshold is exceeded, the system should change to hard-switching mode. Then, the entire data stream will be transmitted either via UOWC ($\alpha = 0$), if the salinity is high, or via MI ($\alpha = 1$) if the turbidity intensifies. Finally, the soft-switching mode can be chosen if both the MI and the UOWC channel exhibit good properties, i.e., if the salinity as well as the turbidity are low. A good and realistic example is the open water in the Baltic Sea [114]. There, the influence of seabed turbulence is low and the salinity of about 0.8 % is far below the average value for all oceans ($\approx$ 3.5 %).

TABLE III
PROPERTIES OF OPTICAL BANDPASS FILTERS FOR APPLICATION IN UOWC SYSTEMS.

Property	Colored glass filter	Thin film filter
Passband transmittance	moderate	high
Spectral slope steepness	smooth	steep
AOI dependence	negligible	large
Light structure sensitivity	minor	existing
Variants available	limited	many, customized
Price	cheap	expensive

V. Ambient Light and Interference Suppression

A. Optical Bandpass Filtering

The assumption of a perfectly dark deep ocean, as often used in related literature, is only a special case in UOWC operations. The same applies to operations limited to dark nights. In contrast, it is practically unavoidable that UOWC systems are exposed to ambient sunlight in some form when operated in water depths less than two hundred meters. Sunlight increases the shot noise or may even cause a saturation of the PD. The underwater light field is diverse and depends on many influencing factors like region, season, time, cloudiness, wind and wave status, as well as water depth and water type in terms of absorption and scattering properties. Overcast conditions create diffuse light, wheres a clear sky enables directed sunlight to enter the water surface. Light penetrating the water column is absorbed and scattered along the path. The strength generally decreases with depth and the character increasingly gets diffuse. Of course the viewing direction of the receiver is also important. A detector facing upward may be exposed to orders of magnitude more ambient light than when facing downward or sideways.

Solar radiation is about flat in the spectral range from roughly $450\,\mathrm{nm}$ to $650\,\mathrm{nm}$ in air. Sunlight entering the water column gets filtered, however. In oceanic waters, with increasing depth the blue spectral range survives, whereas in coastal waters the green color range becomes dominant. To prevent the unwanted fractions of ambient light from reaching the detector, an optical bandpass filter can be used. The transmission band or bandwidth should incorporate the major part the spectral emission band of the light source for efficiency reason. In the case of single-color LEDs the emission has an optical bandwidth in the range of $15\,\mathrm{nm}$ to $35\,\mathrm{nm}$ FWHM and is roughly Gaussian shaped. Narrowing the passband of a filter centered to the emitted peak wavelength would of course increase the SNR, but on the other side demands more gain and thus reduces the electrical bandwidth of the amplifier. The main properties of the two dominating filter types, absorptive colored glass filters and thin film interference filters, are given in Table III.

The major drawbacks of colored glass filters are the moderate transmittance and the soft spectral slopes, which make them inefficient. Only a few decibel of SNR improvement can be expected in the optical domain. Thin film filters are superior in this respect, but suffer from shifting the center wavelength as a function of the angle of incidence (AOI). Also, their passband shape degrades at high AOI, as plotted

This article has been accepted for publication in a future issue of this journal, but has not been fully edited. Content may change prior to final publication. Citation information: DOI 10.1109/COMST.2021.3111984, IEEE Communications Surveys & Tutorials

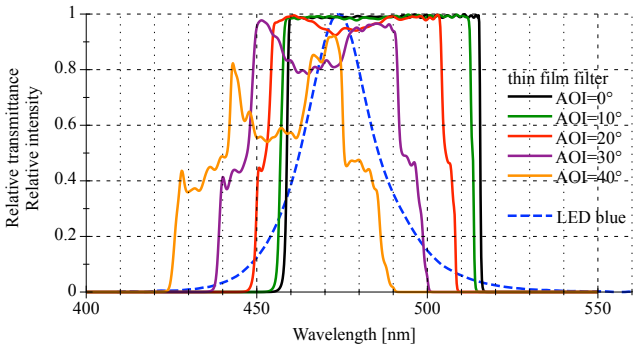

Fig. 21. Relative transmittance of a Semrock FF01-488/50 thin film filter for different angles of incidence as well as the relative intensity of a blue LED Luxeon Lumileds Z. Thin film filter spectra were simulated by Semrock MyLight software. LED spectrum was measured using Gigahertz Optics BTS256 at I_f=350 mA at 25 °C.

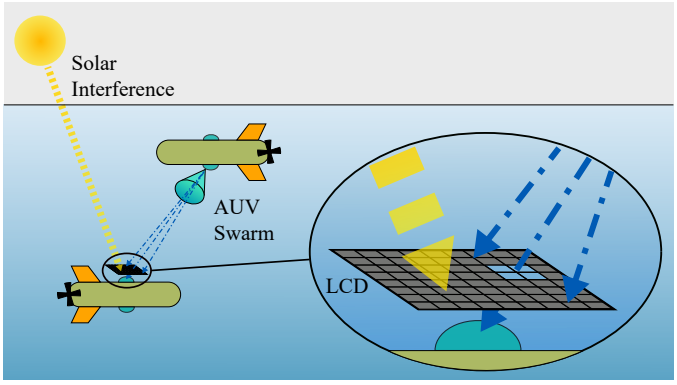

Fig. 22. Illustration of underwater LCD-based interference suppression.

in Fig. 21. Practically, they are only applicable for a FOV up to 60° to 80°. Nevertheless, they are the better choice for UOWC. For more details and examples refer to [115]. Of course thin film filters can be used for wavelength-division multiple access. Considering the available LED colors in the usable spectrum in seawater, only two independent channels (blue and amber) can be established. Allowing less efficiency and minor crosstalk, a third channel in the green regime of the spectrum can additionally be created (see Fig. 5).

Even in the dark ocean other sources of ambient light exist, which can potentially disturb UOWC systems. This can be natural bio-luminescence or artificial light of parallel operated imaging systems for instance. Although when operated at different wavelength bands, fluorescence effects can shift these. If these cases occur, individual filtering needs to be applied.

B. LCD-Based Ambient Light and Interference Suppression

Many contributions to optical underwater communication share a common feature: practical experiments and prototype tests are often conducted in darkened laboratories, thus simplistically assuming a deep-sea scenario or operation at night. As already mentioned in Section V-A, the reason for this assumption is the ambient sunlight, which can severely affect the performance of the communication system. In the worst case, i.e. near the water surface, the PD can be driven into saturation. One possibility to reduce sunlight interference is to employ various types of optical bandpass filters, as shown in the previous section. Another possibility was recently introduced in [98], [100]. There, a static optical bandpass filter is replaced by an LCD acting as a dynamic optical filter to combat ambient light and to decorrelate communication channels in a multi-user scenario.

Generally, LCDs consist of a large number of segments (pixels) containing liquid crystals that are embedded between two polarizing layers. By applying an electric field, the liquid crystals change the polarisation of light, turning segments of the LCD either transparent or non-transparent. As a result, individual pixels as well as whole areas of an LCD can be adjusted to either pass through or block specific light rays. This characteristic makes an LCD well suited for interference cancellation. Initial investigations in [98], [100] have shown that a receiver-side filter setup is desirable, with the LCD positioned at a fixed distance in front of the PD. That way, the FOV of the PD can be focused on a desired signal source while blocking other interfering light beams. When distinguishing between interfering source and desired source, two scenarios must be considered. In the first, the interfering source is unmodulated, like e.g. solar irradiation. Here, the separation is straightforward, since the receiver only needs to be capable of distinguishing between a DC signal and a modulated signal. Once both the interfering and the signal source have been identified, e.g. by sequentially switching different segments of the LCD, those LCD pixels that are in the LOS between the interfering source and the PD can be switched non-transparent, resulting in suppression of the interference. In the second scenario, a modulated interfering source is assumed (cf., small-scale SDMA in Section IV-B). This can either be another communicating light source or a virtual light source, representing a reflected and thus delayed signal component in a multipath scenario. For illustration and simplification purposes, it is presumed in the following that the multipath scenario consists only of the LOS path and one reflection path and that both interfering and signal source are sufficiently spatially separated. It is well known that the reflected signal component in an optical multipath scenario experiences higher attenuation than that from the LOS path. This property can be exploited for interference cancellation with an LCD. Once both sources have been identified by the receiver, those LCD pixels can be switched non-transparent that will suppress the path with the weakest optical power. However, if the modulated interferer turns out to be another communicating light source, separation becomes more difficult. The reason is that now it is no longer sufficient to distinguish between DC and modulated signals or between differences in optical received power. Nevertheless, one example to reliably separate interfering source from signal source is to assign each transmitting light source a unique signature, for instance a semi-orthogonal code as in OCDMA [25], [101]. That way, the receiver can distinguish between different users and the LCD can be adjusted to suppress the undesired source.

As previously mentioned, interference from ambient sun-

This article has been accepted for publication in a future issue of this journal, but has not been fully edited. Content may change prior to final publication. Citation information: DOI 10.1109/COMST.2021.3111984, IEEE Communications Surveys & Tutorials

light is a major challenge in UOWC. Especially near the water surface, strong solar radiation can saturate the receiver and thus severely degrade the communication performance. One possible AUV swarm communication scenario in which this can occur is shown in Fig. 22. Here, the hovering type AUV, which is located near the water surface, transmits data to the going-type AUV, which is located several meters below. However, this exposes the upward-facing receiver of the going AUV to direct sunlight. To prevent this, as a new contribution, LCD-based interference suppression is introduced to AUV swarm communication. Fig. 22 shows a suitable arrangement, in which the LCD is placed at a fixed distance in front of the upward-facing receiver. If the display is then activated as shown in the picture, it is possible with this setup to suppress the interfering sunlight while passing the desired signal from the hovering AUV. Initial investigations in [98], [100] have shown that the interference suppression can reach up to 35 dB for blue-colored LEDs, which are commonly deployed in the underwater environment (cf. Section II-A). Besides the capability to strongly suppress interfering signals, another advantage of an LCD filter for AUV swarm communication is that the display can be considered as a dynamic optical filter. In other words, the LCD can adaptively be adjusted to a varying angle of solar incidence or to position and orientation changes of AUVs.

In this context, however, it is important to point out a fundamental bottleneck of LCD-based interference suppression, namely the low switching frequency of up to 360 Hz for commercially available displays [116]. Therefore, this approach may not be suitable for scenarios involving uncoordinated and/or fast-moving vehicles.

Fortunately, LCD-based interference cancellation is well suited for AUV swarm communication scenarios for the following reasons. First, the typical speed of AUVs over ground is relatively slow at a few knots or less. Therefore, the dwell time of objects within the FoV of the LCD is long enough to detect and track them at reasonable frame rates. Second, the trajectories of vehicles within a swarm are typically coordinated. Therefore, only small relative position changes need to be compensated by the LCD. Last but not least, the position relative to the sun changes only slowly, so the LCD can adjust the blocking area.

VI. Realization Aspects

A. Port and Housing Concepts, Vehicular Integration, and Anti-Biofouling Ultraviolet Illumination

For underwater operations, electronic devices and circuits need to be protected against the surrounding corrosive and conductive seawater. If electro-optical sources or detectors are involved, additionally optical components like windows are indispensable. Fig. 23 presents housing and port concepts for this type of application. Most common and widely used are pressure-resistant cavity housings (A+B), frequently made of aluminum, stainless steel or titanium, but also of (reinforced) plastic. The selection of the material is mainly based on factors like operational depth, strength, weight, corrosion resistance, machinability, and cost. An optical window is integrated into

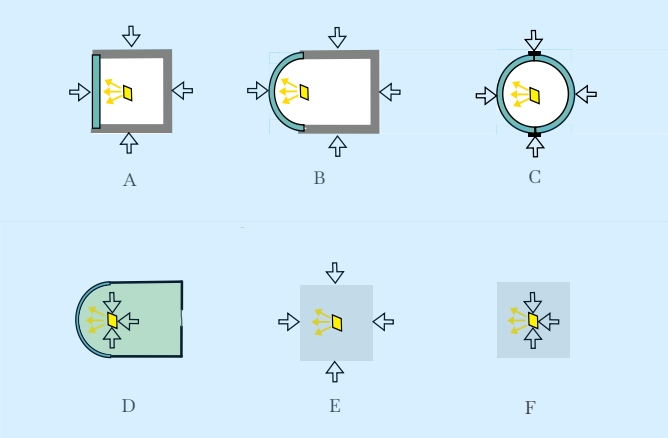

Fig. 23. Typical underwater housing and port concepts for optical devices: (A) pressure housing with flat port and (B) with hemispherical port, (C) glass spherical housing, (D) fluid-filled pressure neutral housing with hemispherical port, (E) pressure-resistant transparent cast, and (F) pressure neutral cast. The hollow arrows are depicting the effect of the pressure of the water column.

the housing, typically a flat port or a dome port. A special case of this type is the spherical glass housing (C), consisting of two precisely fitting hemispheres. Subfigure (D) depicts a fluid-filled thin-walled version of a pressure neutral housing, where the inner components are exposed to the pressure of the water column. Since not all electrical components are pressure resistant, this is limiting the range of usable electronic components. Whereas many semiconductors are usable, capacitors can be problematic. An advantage of (A) to (D) is the general accessibility to the components for service or exchange.

A different way is to embed the components in material like epoxy, polyurethane, or silicon. The process of resin embedding is also known as resin casting or potting in the community. For optical applications, the potting compound must be either transparent or complemented by a small glass window covering the LED or PD, respectively. Depending on the hardness of the potting compound it can be made pressure resistant (E), where the pressure of the water column is withstood by the cast. Embedding of components in softer flexible materials is realized by the pressure neutral concept shown in (F). The concepts of fluid-filling and potting are common and widely used in underwater technology for junction boxes and connectors, but for electro-optical and electronic devices increasing only recently.

Another important aspect is the optical port. The port plays a crucial role in underwater imaging, but in UOWC it is paid less attention [117]. Both the flat and the hemispherical port are usually made of glass or transparent plastics with a refractive index around 1.5. Integrated into a beam path with transitions to water and air, this results in the disadvantage of a restricted FOV for the flat port or a focus-sensitive design for the dome port. The use of lenses and reflectors, commonly designed for the medium air, is straightforward inside a pressure housing, but may be problematic when potted. Heat dissipation is generally not an issue, at least not in metal pressure housings or in thin-walled cast.

The design of omnidirectional optical transmitter and receiver units and their integration into AUVs is challenging.

This article has been accepted for publication in a future issue of this journal, but has not been fully edited. Content may change prior to final publication. Citation information: DOI 10.1109/COMST.2021.3111984, IEEE Communications Surveys & Tutorials

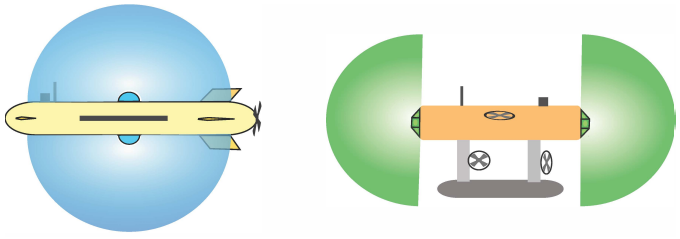

Fig. 24. Possible integration positions for optical hemispherical transducers at two different AUV hulls.

Fig. 25. Prototype of hemispherical transducer in pressure neutral technology, including four sectors of each four power LEDs.

Fig. 26. LED transducer comprising five high-power LED segments and driver electronic individually pressure neutral potted.

Fig. 27. Optical transceiver comprising five high-power LED arrays and a PD with a TIA circuit in the center. The transceiver is installed in a pressure housing with flat port (Fig. 23 (A)).

The majority of AUVs are of torpedo type, this means a narrow cylinder with propulsion aft and a certain minimum speed for stable control. Other designs like flat-hull or multi-hull or open-frame types with hovering capabilities are rare in the field, however. One fundamental idea of AUV swarms is the division into dedicated tasks to avoid all vehicles to be equipped with all types of sensors. This keeps size and cost down, so most likely in the near future swarms will consist of small to medium sized AUVs, rather than large deep sea vehicles. For inter-swarm communication spherical characteristics of transmitting and receiving light are required. Blocking by the hull can be eliminated by splitting the transducers in upper-lower or bow-stern for example, but minor shadowing by fins or antennas cannot be avoided entirely in all cases. Examples are shown in Fig. 24.

Splitting into more smaller sections would increase housing and cabling effort. Towing of a spherical system would be impractical for deployment and recovery of the vehicle and also suffer from blocking by the hull. The energy budget of AUVs is crucial and generally very tight. The power consumption of UOWC systems in small to mid size AUVs is in the range between a few to tens of watts. Higher consumptions would have less acceptance since they are reducing the operational duration severely. Although the typical speed of AUVs is only a few knots, the hydrodynamic design is very important to keep the drag low for high power efficiency of the drive train and the vehicles stability, particularly for torpedo-shaped vehicles. Therefore, the shape of communication transducers need to be as small and streamlined as possible. Another critical design factor is the buoyancy, because small vehicles are very trim and payload sensitive. Even the mechanical robustness is an important property, since glass or plastic thin-walled domes are far more vulnerable than solid potted solutions, as shown in Fig. 25 and Fig. 26. When integrating a UOWC system into the AUVs tight space, the number of cables and connectors, their thickness and routing also need to be considered.

The constraints with respect to shape, volume and power, the requirements regarding the optical characteristics, as well as the possibility of MIMO processing must be matched with the necessary hardware components. The selection of single-color power LEDs, optics, large-area photodetectors and optical bandpass filters is often characterized by compromises, due to the fact of a limited product range in these segments. Factually, this results in dome ports with a diameter on the order of 100 mm or truncated pyramids of about the same dimension with up to ten sectors. When achieving a hemispherical characteristic by combining a number of conical sectors, which are bounded by the beam angle respectively the FOV, overlapping zones are created automatically. The simultaneous use of such neighbouring sectors gives the possibility of applying SIMO or MIMO technology.

Biofouling can be a severe problem for long-term underwater deployment of optical devices. This is due the growing biofilm and thereby decreasing transmittance of light through transparent components like windows, lenses or ports. Depending on environmental conditions like availability of nutrients, water temperature and sunlight, under worst-case circumstances biofouling can occur within hours and in depth up to a few hundred meters. This issue can be solved by using UVC LEDs [106]. The most effective wavelength for antifouling applications is in the band of $250\,\mathrm{nm}$ to $280\,\mathrm{nm}$, therefore utilized window materials need to have a high transmittance in this range. This is the case for fused-silica quartz glass.

B. Simultaneous Illumination and Communication/Localization

One of the key motivations of terrestrial VLC is the fact that light can be used simultaneously for illumination as well as for communication and/or positioning purposes [20]–[25]. Due to this dual/triple functionality, no additional power supply is necessary for data transmission and localization. Correspondingly, CO_2 emission is reduced. In the area of UOWC, for the first time we suggest to use the light source traditionally used

This article has been accepted for publication in a future issue of this journal, but has not been fully edited. Content may change prior to final publication. Citation information: DOI 10.1109/COMST.2021.3111984, IEEE Communications Surveys & Tutorials

for illumination in underwater camera recordings simultaneously also for communication and/or positioning. That way, the operation time of the underwater vehicle can be expanded. VLC is possible both with permanently modulated light as well as light pulses. For instance, given an RGB light source only blue and green are used for communication/localization, whereas red is additively mixed for proper color rendering. For short-range applications it is also possible to use a wideband light source. In [118], multispectral imaging employing just a gray camera is proposed. The trick is that the different colors of an LED-based wideband light source are flashed successively. This smart illumination principle can be extended to include communication/localization functionality by employing spatial modulation [99].

C. Prototypes and Commercial Optical Underwater Modems

Research and development in the field of underwater optical communication has started almost two decades ago. However, the range of commercial products is still relatively small. This is probably due to the special application area and the technical challenges. Table IV provides an overview of available commercial systems and compares the basic specifications and capabilities of these systems. It is remarkable that all systems use LEDs as a light source. To the best knowledge of the authors no laser-based system is available on the market. Generally, all these systems are intended for tether-free connections of an AUV or ROV with some sub sea structure like a lander to transfer stored sensor or video data. Some of the systems are quoting network capabilities, but multiple inter-vehicle communication is not specified in any case. Range and data rate performance figures are clearly stated as maximum values and are subject to change with water quality and ambient light conditions. The applied housing and optical port concepts are quite different. Regarding the size, most systems are designed for ROV usage rather than AUV integration.

In recent times, numerous research groups have presented UOWC prototypes, many of which are mentioned in [40], [45]. In this paper, we want to focus on two new prototypes that pursue fundamentally different design and application approaches. Fig. 27 shows a UOWC prototype comprising five royal blue, high-power LED arrays, which are centered around a large-area PD placed on a TIA circuit board. The transceiver is installed in a pressure housing with flat port (Fig. 23 (A)), which can sustains pressure of up to 15 bar. Behind the transceiver, inside the cylindrical housing, the LED drivers, the microcontroller, and the batteries are accommodated. The aim of this prototype is to optimize power dissipation by applying CSIM modulation (cf. Section III-D). Theoretical predictions could be verified.

Another UOWC prototype is currently being developed within the scope of the research project MAUS (Mobile Autonomous Underwater System) [123]. Within this project, a hovering-type AUV ("Hansel") and a going-type AUV ("Gretel") are designed. These AUVs are equipped with different sensors. By means of bidirectional communication within this team of vehicles, tasks shall be completed jointly. Towards this goal, triple hybrid communication consisting of acoustic, optical, and magneto-inductive data transfer as well as swarm localization are targeted. Fig. 26 shows the LED-based transmitter comprising five high-power LEDs that are individually encapsulated and equipped with an optical concentrator. To achieve improved angular coverage, a dedicated LED carrier was CNC-milled from seawater-resistant aluminium (AlMg3) that allows the outer four LEDs to be positioned at an angle. That way, a communication link can be established even if transmitter and receiver are misaligned, e.g. due to strong currents. Another special feature of this carrier is the hollow structure, which makes it possible to cool the high-power LEDs with seawater. The LED driver unit is encapsulated separately in thermally conductive compound and is mounted below the LED carrier. Consequently, this design corresponds to housing type (F). The receiver unit (not shown in the picture) consists of five modules with large-area PDs placed on TIA circuit board. Each module is individually encapsulated and integrated streamlined into the AUV hull. Evidently, the goal of this prototype is to provide a weight- and footprint-optimized, yet powerful optical communication system. Both optical Tx and Rx units are integrated into each AUV type to enable bidirectional UOWC.

D. Underwater Swarm Projects

In recent time, quite a number of underwater swarm projects have been reported [40], [45]. Some of these include, without claim of completeness, CoCoRo, DeepSeaMining, ESONET, HippoCampus, MAUS, MONSUN, MONSUN II, MORPH, SEMBIO, SMIS, Suave, SUNRISE, SWARMS, Venus Swarm, VERTEX, WiMUST, Zeno AUV (in alphabetic order). To establish an AUV swarm, inter-vehicle communication is essential. So far, the communication is predominately based on acoustics. This is comprehensible, because this technology is field-proven, reliable, and available off-the-shelf. The strength of achieving communication over long distances and a ranging functionality stands opposite to the major disadvantage of limited speed. To date, the demand for fast underwater communication has obviously been at data transfer between two points, generally one fixed like a node on an anchored structure and one at a vehicle like ROV or AUV, so-called data muling. For this application several commercial product are available, see Table IV.

Despite the impressive number of swarm projects, projects where optical communication has been integrated to AUVs targeting swarm communication are rare. One of the first is the CoCoRo underwater swarm project [124]. At this point also the EU project SUNRISE [125] should be mentioned, which was carried out from 2013 to 2016. It was offering extensive infrastructure like testbeds and various AUVs to provide Internet of Underwater Things (IoUT) functionality. This project included acoustical and sophisticated optical communication for mobile nodes as well as swarm technologies, but without establishing optical inter-vehicle communication. In [126] the Venus AUV as of 2018 is described, comprising hybrid technology including acoustic and optical modems. A future test with multiple vehicles in a swarm is planned.

This article has been accepted for publication in a future issue of this journal, but has not been fully edited. Content may change prior to final publication. Citation information: DOI 10.1109/COMST.2021.3111984, IEEE Communications Surveys & Tutorials

TABLE IV
OVERVIEW OF COMMERCIAL UOWC SYSTEMS AVAILABLE ON THE MARKET.

Manufacturer	Aquamodem	Hydromea	Hydromea	Hydromea	Hydromea	Marinelink	Sonardyne	Sonardyne	Sonardyne
Type	OP2	Luma 100	Luma 250LP	Luma 500ER	Luma X	WOCS 40220	Bluecomm 100	Bluecomm 200	Bluecomm 200UV
Tx type	LED	LED	LED	LED	LED	LED	LED	LED	LED, UVA
Rx type	N/A	N/A	N/A	N/A	N/A	APD	PIN PD	PMT	PMT
Range	1 m	2 m	7 m	50 m	50 m	10 m	15 m	150 m	75 m
Data rate	80 kbps	115 kbps	250 kbps	500 kbps	10 Mbps	25 Mbps	5 Mbps	10 Mbps	10 Mbps
Port	flat	flat, potted	flat, potted	flat, potted	flat	dome	dome	dome	dome
Depth rating	3500 m	6000 m	6000 m	6000 m	6000 m	1000 m	4000 m	4000 m	4000 m
Interface	serial	serial	serial	serial	serial, Ethernet	Ethernet	Ethernet	Ethernet	Ethernet
Networking	N/A	N/A	N/A	optional	optional	✓	N/A	N/A	N/A
Acoustic hybrid	N/A	N/A	N/A	N/A	N/A	N/A	optional	optional	optional
Consumption	N/A	5 W	5 W	5 W	5 W	50 W	30 W	25 W	40 W

Data from a survey as of 2021, extracted from [119]–[122], with no claim to completeness and correctness.

The MAUS project [123], which has been introduced in Section VI-C, exploits the potentials of a team of differently equipped AUVs.

VII. SUMMARY AND PERSPECTIVES

A. Conclusions and Lessons Learned

Autonomous underwater swarm robotics is an interdisciplinary topic currently receiving strong interest. In the previous decade, considerable progress has been achieved in various disciplines, including energy storage, underwater sensoring, signal processing, and cooperative underwater navigation. Still, one of the most challenging tasks in mobile underwater swarm robotics is high-speed yet reliable inter-vehicle communication. Besides high-rate communication between AUVs, wideband connection to seafloor infrastructure and surface equipment is challenging. The underwater channel is known to be a harsh environment, even more if transmitters and/or receivers are not stationary. Most wireless underwater communication modems are based on sound waves, but acoustic communication is troublesome for several reasons, particularly in swarm robotics.

In this tutorial, emphasis is on UOWC between mobile nodes. Compared to acoustic modems, much higher data rates are potentially achievable at short ranges and reasonable visibility. The scope of this tutorial is to provide a comprehensive overview of UOWC technologies that are suitable for use in agile robotic swarms. For this reason, only LED-based methods are taken into account since collimated laser beams suffer from a pointing, acquisition, and tracking problem. Precise and small-scale pointing, acquisition and tracking systems are not available on the market yet.

The introduction in Section I provides a background on AUVs and AUV swarms, gives an overview on communication techniques and topologies in underwater swarm robotics, and reports about related overview papers.

Section II deals with channel modeling. Besides the physical channel based on noncoherent light, the impact of LEDs, photodetectors, as well as amplifiers is considered in conjunction with channel modeling. The following lessons can be learned: (i) The wavelength regime, where the attenuation is smallest, depends on the water type. The narrow optical window is particularly challenging in swarm applications requiring many spectral windows; (ii) The green-yellow gap, determined by a poor quantum efficiency of standard semiconductor LEDs in this wavelength range, is particularly disadvantageous in coastal waters. Converted color types partly solve this problem, but at the cost of reduced switching speed; (iii) Unlike laser links, less collimated and shorter ranging LED-based systems are less affected by turbulence; (iv) Regarding photodetectors suitable for UOWC, a trade-off between sensitivity and junction capacitance exists; (v) A careful circuit design of the TIA is necessary in order to provide the highest possible SNR.

In Section III, physical layer transmission techniques are studied. Emphasis is on modulation schemes with two amplitude levels, and on the superposition of square-wave signals. Towards this goal, the novel framework of rectification is proposed. The time, frequency, and spatial domains are taken into account. The positive impact of modulation schemes with a large peak-to-average power ratio is stressed. Also, the advantage of optical frontends employing multiple photodetectors rather than multiple light sources is highlighted. Since energy saving is of utmost importance, rate-adaptive and power-adaptive adaptation strategies are discovered. Constrained superposition coding is a hardware-friendly modulation scheme particularly suitable for the requirements of UOWC swarm communication. The section concludes with channel coding, equalization, and detection aspects. Among the lessons learned are: (i) In the literature it is often overlooked that the received power in the electrical domain is proportional to the average-power-to-squared-mean ratio κ. Hence, the larger κ, the better is the power efficiency of the intensity modulation scheme given the same received power in the optical domain; (ii) Regarding single-carrier modulation schemes, two-level waveforms with adjustable duty cycle are proposed. VPSK, VFSK, and VOOK seem to be novel; (iii) A novel method to realize multicarrier modulation schemes is suggested, where sine/cosine functions are replaced by corresponding rectified waveforms; (iv) Constrained superposition intensity modulation is suitable for multiuser MIMO

processing in UOWC swarms because it is simple yet power efficient; (v) Traditionally, several LEDs are implemented in optical heads in order to boost the intensity and hence the range. We prove that it is superior to use a single LED in conjunction with several photodetectors instead; (vi) Three different forms of cognitive intelligence are discussed: power allocation and adaptive bit loading, reliability-based channel adaptation, and backscattering-based channel adaptation. Cognitive intelligence is particularly helpful in harsh environments and in swarms; (vii) Concerning channel coding, the capabilities of hybrid ARQ, network coding, line coding, bit-interleaved coded modulation, and soft-input soft-output decoding are frequently overlooked in UOWC applications; (viii) Regarding equalization, simple techniques like a guard interval are pointed out to be sufficient in many UOWC scenarios. As an alternative, precoding is suggested for future work.

Data link layer aspects are studied in Section IV. Approaching this goal, duplexing, multiuser, and multihop strategies are presented. Of special practical interest are hybrid transmission schemes, since UOWC is restricted to short ranges. Emphasis is on a combination of acoustic, optical, and magnetic communication. Like UOWC, magnetic communication is also a short-range communication technique, but does not suffer from visibility constraints. Among the lessons learned are: (i) Traditional multiple access schemes like TDMA, FDMA/OFDMA/WDMA, SDMA, and OCDMA are outperformed by non-orthogonal multiple access schemes, including IDMA, at the expense of an increased receiver complexity; (ii) The communication range can be increased by multihop transmission and relaying; (iii) In environments with poor or time-varying visibility, UOWC can be complemented or substituted by magnetic communication for improved quality of service. Hybrid optic/magnetic near-range communication is proposed to complement long-range acoustic communication. Acoustic communication can be seen as an umbrella cell, covering several local optic/magnetic communication cells; (iv) In magnetic communication, the receiver coil can be replaced by a high-sensitive wideband magnetic field sensor.

Section V deals with ambient light and interference suppression – topics which are rarely considered in the underwater communications community so far. Focus is on optical bandpass-filter-based as well as on LCD-based techniques. In the latter case, the pixels of a liquid crystal display are used as an adaptive optical aperture for ambient light and/or interference mitigation. Novel aspects include: (i) With optical bandpass filtering, the number of communication channels can be increased. Furthermore, ambient light can be suppressed. Best results have been obtained for thin film filters; (ii) Liquid crystal arrays are, besides ambient light suppression, additionally useful for interference mitigation in slowly time-varying scenarios, because they are adaptive. This feature is of particular interest in swarm communication with coordinated nodes. Still, more work in this area needs to be done.

In Section VI, realization aspects are subsumed. The section starts with port and housing concepts, vehicular integration, and anti-biofouling ultraviolet illumination for long-term missions. Pressure-neutral potting is an advanced yet cheap housing technology that is particularly tailored to robotic swarms with small vehicles. For the first time, simultaneous illumination and communication/localization exploiting underwater camera lighting is discussed. Finally, a survey on optical underwater modems and on underwater swarm projects is presented. These realization aspects have never been presented in UOWC overview papers before.

B. Outlook

Although there has been a lot of progress on UOWC and hybrid technologies in the previous decade, there are still areas that are not mature, c.f. Table V. Of utmost importance, perhaps, is the need for more practical experience and applications. On the one hand, most UOWC modems have not been designed for AUVs applications. On the other hand, fully-autonomous AUV swarm technology suitable for long-distance and long-term missions is not ready for the market yet. The process of commercialization not only requires further measurement campaigns, but could also become more sustainable through the standardization of communication systems. Generally accepted underwater reference channel models would be helpful, similar to established channel models in terrestrial wireless radio communication, so that communication equipment from different manufacturers can be compared on a fair basis. Along the same lines, standardization of UOWC communication systems would ease commercialization.

At the physical layer, improvement of energy and bandwidth efficiencies are most important. Software-defined radio and cognitive radio implementations should be guided by an advanced optical head concept, employing smart, adaptive, and intelligent hybrid transceivers.

Essentially, the communication network of interest is a vehicular ad hoc network. In the case of hybrid communication, it is even a heterogeneous vehicular ad hoc network. Software-defined networking is a possible solution to related challenges [127], targeting improved (massive) connectivity, reduction of latency, and quality of service provisioning. Continuous and worldwide access to all swarm elements would provide extra benefits for operators, but is a huge challenge.

Precise underwater localization still deserves future research and development. With cooperative localization the inaccuracies of the motion reference unit and the inertial navigation unit can be reduced [128]. In cooperative localization, range estimates between mobile nodes and fixed anchors, if available, are exchanged and processed either centralized or decentralized. Although UOWC is a short-range technique, it is helpful for data exchange in cooperative localization, as the distances inside a swarm can be controlled. Range estimates are usually more precise with optical signaling because of LOS propagation and much shorter wavelengths.

Another enabling topics is swarm control. Although the fundamentals have been established (see [129] and references therein), practical tests in the harsh underwater environment are pending. In this context it is important to mention that communication signals are simultaneously re-usable for localization purposes in order to economize on power and bandwidth. Compared to acoustic communication, in UOWC

TABLE V
OVERVIEW OF FUTURE RESEARCH TOPICS ON UOWC-ASSISTED AUV SWARMS.

Topic	Research goal
Standardization	Definition of reference UOWC channel models and standardization of UOWC communication systems
Physical layer	Improvement of energy and bandwidth efficiencies; smart, adaptive, and intelligent hybrid transceivers
Upper layers	Software-defined networking; Improved connectivity; reduction of latency; quality of service provisioning
Localization	Cooperative localization; joint communication and localization
Swarm intelligence & control	Automated swarm control, driven by artificial intelligence and machine learning
Security	Physical layer security & network coding in underwater robotic swarms
Energy supply	Energy harvesting; advanced docking stations with bidirectional data transfer
Practical experience	Field tests including environmental data for superior channel modeling; long-term campaigns; commercialization

the control functionality is not degraded by the propagation delay of the channel. A related topic is swarm intelligence [130]. Artificial intelligence (AI) and machine learning (ML) [131] may pave the road to swarm intelligence and fully-automated swarm control. Potential additional applications of AI and ML include intelligent underwater data acquisition, big data analysis, and cognitive communication functionality, among others.

Once underwater swarm technology has reached a commercial level, security issues will get important. Towards this goal, network coding and physical layer security [132] provide interesting features suitable for robotic swarms. Light communication relaxes the general security problem, because it is more eavesdrop secure, difficult to jam, and quasi delayless.

Last but not least, long-term deployment of AUV swarms is desirable. In deep-sea AUV missions, the daily cost of the escorting research vessel is on the order of several USD 10,000. Besides this cost argument, discontinuous operation is not time efficient and data gaps may occur. Above moderate sea states the cost/efficiency problems are particularly troublesome. AUV swarms are even more difficult to handle by external support. Underwater docking stations relax the mentioned problems [133], possibly in connection with energy harvesting. On the uplink, collected data could be uploaded to the docking station. If the docking station is equipped with a surface or shore cable, the access time to recover the collected data is shortened, since high-speed data excess to the outside world is typically not available for an AUV unless it is surfaced. Vice versa, on the downlink the AUV batteries could be re-charged and a new mission schedule could be downloaded from the docking station. UOWC can be used for short-range data exchange between AUV and docking station, but also for guiding the docking process.

Acknowledgement

This work has been partly supported by the European Union – European Regional Development Fund (ERDF), the Federal Government and Land Schleswig-Holstein, Germany, through EU.SH Project, under Grant LPW-E/1.2.2/1075. The authors would like to thank the anonymous reviewers for constructive comments that improved the quality of the manuscript.

REFERENCES

[1] Market and Markets, "Autonomous Underwater Vehicle (AUV) Market by Type (Shallow AUVs, Medium AUVs, Large AUVs), Application (Military & Defense, Oil & Gas), Shape, Technology (Navigation, Imaging), Payload Type (Cameras, Sensors), Region – Global Forecast to 2025," Apr. 2020, report Code SE 3671.
[2] N. Vedachalam, R. Ramesh, V. B. N. Jyothi, V. D. Prakash, and G. A. Ramadass, "Autonomous underwater vehicles – challenging developments and technological maturity towards strategic swarm robotics systems," *Marine Georesources & Geotechnology*, pp. 1–12, Apr. 2018.
[3] http://www.auvac.org, accessed: 2021-03-20.
[4] http://robotdirectory.auvsi.org, accessed: 2021-03-20.
[5] J. Connor, B. Champion, and M. A. Joordens, "Current algorithms, communication methods and designs for underwater swarm robotics: A review," *IEEE Sensors*, vol. 21, no. 1, pp. 153–169, Jan. 2021.
[6] L. Bayindir, "A review of swarm robotics tasks," *Neurocomputing*, vol. 172, pp. 292–321, Jan. 2016.
[7] E. M. Sozer, M. Stojanovic, and J. G. Proakis, "Underwater acoustic networks," *IEEE Journal of Oceanic Engineering*, vol. 25, no. 1, pp. 72–83, Jan. 2000.
[8] M. Stojanovic and J. Preisig, "Underwater acoustic communication channels: Propagation models and statistical characterization," *IEEE Communications Magazine*, vol. 47, no. 1, pp. 84–89, Jan. 2009.
[9] X. Lurton, *An Introduction to Underwater Acoustics: Principles and Applications.* Springer, 2002.
[10] R. J. Urick, *Principles of Underwater Sound*. Peninsula Publishing, 2013.
[11] R. Istepanian and M. Stojanovic (Eds.), *Underwater Acoustic Digital Signal Processing and Communication Systems.* Springer, 2013.
[12] S. Hranilovic, *Wireless Optical Communication Systems*. Springer, 2005.
[13] R. Ramirez-Iniguez, S. M. Idrus, and Z. Sun, *Optical Wireless Communications: IR for Wireless Connectivity*. CRC Press, 2008.
[14] S. Arnon, J. Barry, G. Karagiannidis, R. Schober, and M. Uysal (Eds.), *Advanced Optical Wireless Communication Systems*. Cambridge University Press, 2012.
[15] O. Bouchet, *Wireless Optical Communications*. ISTE Ltd, 2012.
[16] D. Chandha, *Terrestrial Wireless Optical Communication*. McGraw-Hill, 2013.
[17] M. Uysal, C. Capsoni, Z. Ghassemlooy, A. Boucouvalas, and E. Udvary (Eds.), *Optical Wireless Communications: An Emerging Technology*. Springer, 2016.
[18] A. K. Majumdar, *Optical Wireless Communications for Broadband Global Internet Connectivity: Fundamentals and Potential Applications*. Elsevier, 2019.
[19] Z. Ghassemlooy, W. Popoola, and S. Rajbhandari, *Optical Wireless Communications: System and Channel Modelling With MATLAB*. CRC Press, 2nd ed., 2019.
[20] S. Arnon (Ed.), *Visible Light Communication*. Cambridge University Press, 2015.
[21] S. Dimitrov and H. Haas, *Principles of LED Light Communications: Towards Networked Li-Fi*. Cambridge University Press, 2015.
[22] Z. Ghassemlooy, L. N. Alves, S. Zvanovec, and M. A. Khalighi (Eds.), *Visible Light Communications: Theory and Applications*. CRC Press, 2017.
[23] Z. Wang, Q. Wang, W. Huang, and Z. Xu, *Visible Light Communications: Modulation and Signal Processing*. John Wiley & Sons, 2017.
[24] N. Chi, *LED-Based Visible Light Communications*. Springer, 2018.
[25] P. A. Hoeher, *Visible Light Communications: Theoretical and Practical Foundations*. Munich: Carl Hanser, 2019.
[26] A. S. Hamza, J. S. Deogun, and D. R. Alexander, "Classification framework for free space optical communication links and systems,"

IEEE Communications Surveys & Tutorials, vol. 21, no. 2, pp. 1346–1382, Second Quarter 2019.

[27] B. M. Cochenour, L. J. Mullen, and A. E. Laux, "Characterization of the beam-spread function for underwater wireless optical communications links," *IEEE Journal of Oceanic Engineering*, vol. 33, no. 4, pp. 513–521, Oct. 2008.

[28] J. Xu, A. Lin, X. Yu, Y. Song, M. Kong, F. Qu, J. Han, W. Jia, and N. Deng, "Underwater laser communication using an OFDM-modulated 520-nm laser diode," *IEEE Photonics Technology Letters*, vol. 28, no. 20, pp. 2133–2136, Oct. 2016.

[29] X. Sun, C. H. Kang, M. Kong, O. Alkhazragi, Y. Guo, M. Ouhssain, Y. Weng, B. H. Jones, T. K. Ng, and B. S. Ooi, "A review on practical considerations and solutions in underwater wireless optical communication," *IEEE/OSA Journal of Lightwave Technology*, vol. 38, no. 2, pp. 421–431, Jan. 2020.

[30] X. Che, I. Wells, G. Dickers, P. Kear, and X. Gong, "Re-evaluation of RF electromagnetic communication in underwater sensor networks," *IEEE Communications Magazine*, vol. 48, no. 12, pp. 143–151, Dec. 2010.

[31] I. I. Smolyaninov, Q. Balzano, C. C. Davis, and D. Young, "Surface wave based underwater radio communication," *IEEE Antennas and Wireless Propagation Letters*, vol. 17, no. 12, pp. 2503–2507, Dec. 2018.

[32] I. F. Akyildiz, P. Wang, and Z. Sun, "Realizing underwater communication through magnetic induction," *IEEE Communications Magazine*, vol. 53, no. 11, pp. 42–48, Nov. 2015.

[33] Y. Li, S. Wang, C. Jin, Y. Zhang, and T. Jiang, "A survey of underwater magnetic induction communications: Fundamental issues, recent advances, and challenges," *IEEE Communications Surveys & Tutorials*, vol. 21, no. 3, pp. 2466–2487, Third Quarter 2019.

[34] M. Hott, P. A. Hoeher, and S. Reinecke, "Magnetic communication using high-sensitive magnetic field detectors," *Sensors 2019*, vol. 19, no. 15, article ID 3415, Aug. 2019.

[35] M. Hott and P. A. Hoeher, "Underwater communication employing high-sensitive magnetic field detectors," *IEEE Access*, vol. 8, pp. 177 385–177 394, Oct. 2020.

[36] M. Hott, A. Harlakin, and P. A. Hoeher, "Hybrid communication and localization underwater network nodes based on magnetic induction and visible light for AUV support," in *Proc. 2020 Int. Conf. Information and Communication Technology Convergence (ICTC)*, Sydney, Australia, Aug. 2020.

[37] J. Joe and S. H. Toh, "Digital underwater communication using electric current method," in *Proc. MTS/IEEE OCEANS 2017*, Aberdeen, UK, Jun. 2017.

[38] W. Wang, J. Liu, G. Xie, L. Wen, and J. Zhang, "A bio-inspired electrocommunication system for small underwater robots," *Bioinspiration & Biomimetics*, vol. 12, no. 3, Mar. 2017.

[39] H. Kaushal and G. Kaddoum, "Underwater optical wireless communication," *IEEE Access*, vol. 4, pp. 1518–1547, Apr. 2016.

[40] Z. Zeng, S. Fu, H. Zhang, Y. Dong, and J. Cheng, "A survey of underwater optical wireless communications," *IEEE Communications Surveys & Tutorials*, vol. 19, no. 1, pp. 204–238, First Quarter 2017.

[41] N. Saeed, A. Celik, T. Y. Al-Naffouri, and M.-S. Alouini, "Underwater optical wireless communications, networking, and localization: A survey," *Ad Hoc Networks*, vol. 94, Nov. 2019.

[42] G. S. Spagnolo, L. Cozzella, and F. Leccese, "Underwater optical wireless communications: Overview," *Sensors 2020*, vol. 20, no. 8, article ID 2261, Apr. 2020.

[43] E. Felemban, F. K. Shaikh, U. M. Qureshi, A. A. Sheikh, and S. B. Qaisar, "Underwater sensor network applications: A comprehensive survey," *International Journal of Distributed Sensor Networks*, vol. 11, no. 11, p. 896832, Nov. 2015.

[44] C. Gussen, P. Diniz, M. Campos, W. Martins, F. Costa, and J. Gois, "A survey of underwater wireless communication technologies," *Journal of Communication and Information Systems*, vol. 31, pp. 242–255, Jan. 2016.

[45] M. F. Ali, D. N. K. Jayakody, Y. A. Chursin, S. Affes, and S. Dmitry, "Recent advances and future directions on underwater wireless communications," *Archives of Computational Methods in Engineering*, vol. 27, pp. 1379–1412, Nov. 2020.

[46] C. D. Mobley, *Light and Water*. Academic Press Inc., 1994.

[47] R. C. Smith and K. S. Baker, "Optical properties of the clearest natural waters (200–800 nm)," *Applied Optics*, vol. 20, no. 2, pp. 177–184, Jan. 1981.

[48] A. Bricaud, M. Babin, A. Morel, and H. Claustre, "Variability in the chlorophyll-specific absorption coefficients of natural phytoplankton: Analysis and parameterization," *Journal of Geophysical Research*, vol. 100, no. C7, p. 13321, Jul. 1995.

[49] A. Bricaud, A. Morel, and L. Prieur, "Absorption by dissolved organic matter of the sea (yellow substance) in the UV and visible domains," *Limnology and Oceanography*, vol. 26, no. 1, pp. 43–53, Jan. 1981.

[50] C. S. Roesler, M. J. Perry, and K. L. Carder, "Modeling in situ phytoplankton absorption from total absorption spectra in productive inland marine waters," *Limnology and Oceanography*, vol. 34, no. 8, pp. 1510–1523, Dec. 1989.

[51] M. Babin, D. Stramski, G. M. Ferrari, H. Claustre, A. Bricaud, G. Obolensky, and N. Hoepffner, "Variations in the light absorption coefficients of phytoplankton, nonalgal particles, and dissolved organic matter in coastal waters around Europe," *Journal of Geophysical Research*, vol. 108, no. C7, Jul. 2003.

[52] V. I. Haltrin, "Chlorophyll-based model of seawater optical properties," *Applied Optics*, vol. 38, no. 33, pp. 6826–6832, Nov. 1999.

[53] T. J. Petzold, "Volume scattering functions for selected ocean waters," Scripps Institution of Oceanography La Jolla Ca Visibility Lab, Tech. Rep. SIO-REF-72-78, Oct. 1972.

[54] C. D. Mobley, L. K. Sundman, and E. Boss, "Phase function effects on oceanic light fields," *Applied Optics*, vol. 41, no. 6, pp. 1035–1050, Feb. 2002.

[55] Y. Baykal, "Scintillations of LED sources in oceanic turbulence," *Applied Optics*, vol. 55, no. 31, pp. 8860–8863, oct 2016.

[56] M. G. Solonenko and C. D. Mobley, "Inherent optical properties of Jerlov water types," *Applied Optics*, vol. 54, no. 17, pp. 5392–5401, Jan. 2015.

[57] E. F. Schubert, *Light Emitting Diodes*. E. Fred Schubert, 3rd ed., 2018.

[58] J. Sticklus, P. A. Hoeher, and R. Roettgers, "Optical underwater communication: The potential of using converted green LEDs in coastal waters," *IEEE Journal of Oceanic Engineering*, vol. 44, no. 2, pp. 535–547, Apr. 2019.

[59] P. Tian, X. Liu, S. Yi, Y. Huang, S. Zhang, X. Zhou, L. Hu, L. Zheng, and R. Liu, "High-speed underwater optical wireless communication using a blue GaN-based micro-LED," *Optics Express*, vol. 25, no. 2, Jan. 2017.

[60] N. E. Farr, C. T. Pontbriand, J. D. Ware, and L.-P. A. Pelletier, "Non-visible light underwater optical communications," in *Proc. 3rd IEEE Underwater Communications and Networking Conference (UComms)*, Lerici, Italy, Aug 2016.

[61] P. Leon, F. Roland, L. Brignone, J. Opderbecke, J. Greer, M. A. Khalighi, T. Hamza, S. Bourennane, and M. Bigand, "A new underwater optical modem based on highly sensitive silicon photomultipliers," in *Proc. MTS/IEEE OCEANS 2017*, Aberdeen, UK, Jun. 2017.

[62] J. Sticklus, P. A. Hoeher, and M. Hieronymi, "Experimental characterization of single-color power LEDs used as photodetectors," *Sensors 2020*, vol. 20, no. 20, article ID 5200, Sep. 2020.

[63] J. W. Giles and I. N. Bankman, "Underwater optical communications systems. Part 2: Basic design considerations," in *Proc. 2005 IEEE Military Communications Conference*, Atlantic City, NJ, USA, Oct. 2005.

[64] M. Doniec, M. Angermann, and D. Rus, "An end-to-end signal strength model for underwater optical communications," *IEEE Journal of Oceanic Engineering*, vol. 38, no. 4, pp. 743–757, Oct. 2013.

[65] B. Cochenour and L. Mullen, "Channel response measurements for diffuse non-line-of-sight NLOS optical communication links underwater," in *Proc. MTS/IEEE OCEANS 2011*, Waikoloa, HI, USA, Sep. 2011.

[66] F. Jasman and R. J. Green, "Monte Carlo simulation for underwater optical wireless communications," in *Proc. 2nd Int. Workshop on Optical Wireless Communications (IWOW)*, Newcastle Upon Tyne, UK, Oct. 2013, pp. 113–117.

[67] S. Arnon and D. Kedar, "Non-line-of-sight underwater optical wireless communication network," *Opt. Soc. Am. A*, vol. 26, no. 3, pp. 530–539, Mar. 2009.

[68] https://tools.analog.com/en/photodiode/, accessed: 2021-02-10.

[69] H. Schulze, "Some good reasons for using OFDM in optical wireless communications," in *Proc. Int. OFDM Workshop*, Hamburg, Germany, Aug./Sep. 2011.

[70] M. Zhang and Z. Zhang, "An optimum DC-biasing for DCO-OFDM system," *IEEE Communications Letters*, vol. 18, no. 8, pp. 1351–1354, Aug. 2014.

[71] S. D. Dissanayake and J. Armstrong, "Comparison of ACO-OFDM, DCO-OFDM and ADO-OFDM in IM/DD systems," *IEEE/OSA Journal of Lightwave Technology*, vol. 31, no. 7, pp. 1063–1072, Apr. 2013.

[72] S. C. J. Lee, S. Randel, F. Breyer, and A. M. J. Koonen, "PAM-DMT for intensity-modulated and direct-detection optical communication systems," *IEEE Photonics Technology Letters*, vol. 21, no. 23, pp. 1749–1751, Dec. 2009.

[73] J. Armstrong, "OFDM for optical communications," *IEEE/OSA Journal of Lightwave Technology*, vol. 27, no. 3, pp. 189–204, Feb. 2009.

[74] T. Fath, C. Heller, and H. Haas, "Optical wireless transmitter employing discrete power level stepping," *IEEE/OSA Journal of Lightwave Technology*, vol. 31, no. 11, pp. 1734–1743, Jun. 2013.

[75] M. S. A. Mossaad, S. Hranilovic, and L. Lampe, "Visible light communications using OFDM and multiple LEDs," *IEEE Transactions on Communications*, vol. 63, no. 11, pp. 4304–4313, Nov. 2015.

[76] G. J. M. Forkel and P. A. Hoeher, "Constrained intensity superposition: A hardware-friendly modulation method," *IEEE/OSA Journal of Lightwave Technology*, vol. 36, no. 3, pp. 658–665, Feb. 2018.

[77] P. Hoeher, S. Kaiser, and P. Robertson, "Two-dimensional pilot-symbol-aided channel estimation by Wiener filtering," in *Proc. IEEE Int. Conf. on Acoustics, Speech, and Signal Processing (ICASSP '97)*, Munich, Germany, Apr. 1997, pp. 1845–1848.

[78] P. Robertson, P. Hoeher, and E. Villebrun, "Optimal and sub-optimal maximum a posteriori algorithms suitable for turbo decoding," *European Transactions on Telecommunications*, vol. 8, no. 2, pp. 119–125, Mar./Apr. 1995.

[79] J. C. Fricke, M. M. Butt, and P. A. Hoeher, "Quality-oriented adaptive forwarding for wireless relaying," *IEEE Communications Letters*, vol. 12, no. 3, pp. 200–202, Mar. 2008.

[80] J. C. Fricke and P. A. Hoeher, "Reliability-based retransmission criteria for hybrid ARQ," *IEEE Transactions on Communications*, vol. 57, no. 8, pp. 2181–2184, Aug. 2009.

[81] R. A. Maffione and D. R. Dana, "Instruments and methods for measuring the backward-scattering coefficient of ocean waters," *Appl. Opt.*, vol. 36, no. 24, pp. 6057–6067, Aug. 1997.

[82] J. Simpson, B. Hughes, and J. Muth, "Smart transmitters and receivers for underwater free-space optical communication," *IEEE Journal on Selected Areas in Communications*, vol. 30, no. 5, pp. 964–974, Jun. 2012.

[83] J. Sullivan, M. Twardowski, J. Zaneveld, and C. Moore, "Measuring optical backscattering in water," *Light Scattering Reviews 7*, pp. 189–224, Aug. 2013.

[84] S. Lin and D. J. Costello, *Error Control Coding: Fundamentals and Applications*. Pearson/Prentice-Hall, 2nd ed., 2004.

[85] W. E. Ryan and S. Lin, *Channel Codes: Classical and Modern*. Cambridge University Press, 2009.

[86] T. K. Moon, *Error Correction Coding: Mathematical Methods and Algorithms*. Wiley, 2020.

[87] S. B. Wicker and V. K. Bhargava (Eds.), *Reed-Solomon Codes and their Applications*. IEEE Press, 1994.

[88] T. Richardson and R. Urbanke, *Modern Coding Theory*. Cambridge University Press, 2008.

[89] O. Gazi, *Polar Codes: A Non-Trivial Approach to Channel Coding*. Springer, 2019.

[90] C. Schlegel and L. Perez, *Trellis and Turbo Coding*. Wiley, 2004.

[91] A. Shokrollahi and M. Lubi, *Raptor Codes*. now Publishers, 2011.

[92] Z. Guo, B. Wang, P. Xie, W. Zeng, and J.-H. Cui, "Efficient error recovery with network coding in underwater sensor networks," *Ad Hoc Networks*, vol. 7, p. 791–802, 2009.

[93] M. Médard and A. Sprintson, *Network Coding: Fundamentals and Applications*. Academic Press, 2012.

[94] R. E. Ziemer and W. H. Tranter, *Principles of Communications*. Wiley, 7th ed., 2014.

[95] A. Guillén i Fabregàs, A. Martinez, and G. Caire, *Bit-Interleaved Coded Modulation*. now Publishers, 2018.

[96] P. A. Hoeher and T. Wo, "Superposition modulation: Myths and facts," *Communications Magazine*, vol. 49, no. 12, pp. 110–116, Dec. 2011.

[97] J. G. Proakis and M. Salehi, *Digital Communications*. McGraw-Hill, 5th ed., 2008.

[98] A. Krohn, G. J. M. Forkel, P. A. Hoeher, and S. Pachnicke, "LCD-based optical filtering suitable for non-imaging channel decorrelation in VLC applications," *IEEE/OSA Journal of Lightwave Technology*, vol. 37, no. 23, pp. 5892–5898, Dec. 2019.

[99] R. Mesleh, H. Haas, S. Sinanovic, C. W. Ahn, and S. Yun, "Spatial modulation," *IEEE Transactions on Vehicular Technology*, vol. 57, no. 4, pp. 2228–2241, Jul. 2008.

[100] G. J. M. Forkel, A. Krohn, and P. A. Hoeher, "Optical interference suppression based on LCD-filtering," *Applied Sciences*, vol. 9, no. 15, Aug. 2019.

[101] J. Salehi, B. Ghaffari, and M. Matinfar, *Wireless Optical CDMA Communication Systems*. Cambridge University Press, 2012.

[102] L. Ping, "Interleave division multiple-access," *IEEE Transactions on Wireless Communications*, vol. 5, no. 4, pp. 938–947, Apr. 2006.

[103] Y. Liu, Z. Qin, and Z. Ding, *Non-Orthogonal Multiple Access for Massive Connectivity*. Springer, 2019.

[104] M. A. Kashani, M. M. Rad, M. Safari, and M. Uysal, "All-optical amplify-and-forward relaying system for atmospheric channels," *IEEE Communications Letters*, vol. 16, no. 10, pp. 1684–1687, Oct. 2012.

[105] A. Celik, N. Saeed, B. Shihada, T. Y. Al-Naffouri, and M. Alouini, "End-to-end performance analysis of underwater optical wireless relaying and routing techniques under location uncertainty," *IEEE Transactions on Wireless Communications*, vol. 19, no. 2, pp. 1167–1181, Feb. 2020.

[106] J. Sticklus, T. Kwasnitschka, and P. A. Hoeher, "Method and device for potting an LED luminaire potted in a potting compound and LED luminaire," European Patent EP3233414B1, Jan. 2020.

[107] C. Knievel, P. A. Hoeher, and G. Auer, "On the combining of correlated random measures with application to graph-based receivers," *IEEE Communication Letters*, vol. 16, no. 12, pp. 1996–1999, Dec. 2012.

[108] I. Vasilescu, C. Detweiler, M. Doniec, D. Gurdan, S. Sosnowski, J. Stumpf, and D. Rus, "AMOUR V: A hovering energy efficient underwater robot capable of dynamic payloads," *The International Journal of Robotics Research*, vol. 29, no. 5, pp. 547–570, Jan. 2010.

[109] I. Vasilescu, K. Kotay, D. Rus, M. Dunbabin, and P. Corke, "Data collection, storage, and retrieval with an underwater sensor network," in *Proc. 3rd Int. Conf. Embedded Networked Sensor Systems*, New York, NY, USA, Nov. 2005, p. 154–165.

[110] N. Farr, A. Bowen, J. Ware, C. Pontbriand, and M. Tivey, "An integrated, underwater optical/acoustic communications system," in *Proc. MTS/IEEE OCEANS 2010*, Sydney, Australia, May 2010, pp. 1–6.

[111] S. Han, Y. Noh, R. Liang, R. Chen, Y.-J. Cheng, and M. Gerla, "Evaluation of underwater optical-acoustic hybrid network," *China Communications*, vol. 11, no. 5, pp. 49–59, Aug. 2014.

[112] J. Wang, W. Shi, L. Xu, L. Zhou, Q. Niu, and J. Liu, "Design of optical-acoustic hybrid underwater wireless sensor network," *Journal of Network and Computer Applications*, vol. 92, pp. 59–67, Aug. 2017.

[113] F. Janssen, C. Schrum, and J. Backhaus, "A climatological data set of temperature and salinity for the Baltic Sea and the North Sea," *Deutsche Hydrographische Zeitschrift*, vol. 51, pp. 5–245, Oct. 1999.

[114] R. Feistel, W. Stefan, H. Wolf, S. Seitz, P. Spitzer, B. Adel, G. Nausch, B. Schneider, and D. Wright, "Density and absolute salinity of the Baltic Sea 2006–2009," *Ocean Science*, vol. 6, pp. 3–24, Jan. 2010.

[115] J. Sticklus, M. Hieronymi, and P. A. Hoeher, "Effects and constraints of optical filtering on ambient light suppression in LED-based underwater communications," *Sensors 2018*, vol. 18, no. 11, article ID 3710, Nov. 2018.

[116] https://www.digitaltrends.com/computing/asus-rog-swift-360hz-ces-2020, accessed: 2021-05-28.

[117] F. Menna, E. Nocerino, F. Fassi, and F. Remondino, "Geometric and optic characterization of a hemispherical dome port for underwater photogrammetry," *Sensors 2016*, vol. 16, no. 1, article ID 48, Jan. 2016.

[118] H. Liu, J. Sticklus, K. Köser, H.-J. T. Hoving, H. Song, Y. Chen, J. Greinert, and T. Schoening, "TuLUMIS – a tunable LED-based underwater multispectral imaging system," *Optics Express*, vol. 26, no. 6, pp. 7811–7828, Mar. 2018.

[119] https://www.hydromea.com, accessed: 2021-02-17.

[120] https://www.aquatecgroup.com, accessed: 2021-02-17.

[121] https://www.marine-link.com, accessed: 2021-02-17.

[122] https://www.sonardyne.com, accessed: 2021-02-17.

[123] https://www.maus-projekt.de, accessed: 2021-02-19.

[124] T. Schmickl, R. Thenius, C. Moslinger, J. Timmis, A. Tyrrell, M. Read, J. Hilder, J. Halloy, A. Campo, and C. Stefanini, "CoCoRo – The self-aware underwater swarm," in *Proc. 2011 Fifth IEEE Conf. on Self-Adaptive and Self-Organizing Systems Workshops*, Ann Arbor, MI, USA, Oct. 2011, pp. 120–126.

[125] www.fp7-sunrise.eu, accessed: 2021-03-05.

[126] C. Lodovisi, P. Loreti, L. Bracciale, and S. Betti, "Performance analysis of hybrid optical–acoustic AUV swarms for marine monitoring," *Future Internet*, vol. 10, no. 7, pp. 1–13, Jul. 2018.

[127] I. F.Akyildiz, P. Wang, and S.-C. Lin, "Softwater: Software-defined networking for next-generation underwater communication systems," *Ad Hoc Networks*, vol. 46, pp. 1–11, Aug. 2016.

[128] A. Bahr, J. J. Leonard, and M. F. Fallon, "Cooperative localization for autonomous underwater vehicles," *The International Journal of Robotics Research*, vol. 28, no. 6, pp. 714–728, May 2009.
[129] S. Zhang, R. Pöhlmann, T. Wiedemann, A. Dammann, H. Wymeersch, and P. A. Hoeher, "Self-aware swarm navigation in autonomous exploration missions," *Proceedings of the IEEE*, vol. 108, no. 7, pp. 1168–1195, Jul. 2020.
[130] M. G. Hinchey, R. Sterritt, and C. Rouff, "Swarms and swarm intelligence," *Computer*, vol. 40, no. 4, pp. 111–113, Apr. 2007.
[131] K. S. Keerthi, B. Mahapatra, and V. G. Menon, "Into the world of underwater swarm robotics: Architecture, communication, applications and challenges," *Recent Advances in Computer Science and Communications*, vol. 13, no. 2, pp. 110–119, Apr. 2020.
[132] C. Lal, R. Petroccia, K. Pelekanakis, M. Conti, and J. Alves, "Toward the development of secure underwater acoustic networks," *IEEE Journal of Oceanic Engineering*, vol. 42, no. 4, pp. 1075 – 1087, Oct. 2017.
[133] A. M. Yazdani, K. Sammut, O. Yakimenko, and A.Lammas, "A survey of underwater docking guidance systems," *Robotics and Autonomous Systems*, vol. 124, p. 103382, Feb. 2020.

Peter Adam Hoeher (F'14) received the Dipl.-Ing. (M.Sc.) degree in electrical engineering from RWTH Aachen University, Aachen, Germany, in 1986, and the Dr.-Ing. (Ph.D.) degree in electrical engineering from the University of Kaiserslautern, Kaiserslautern, Germany, in 1990. From 1986 to 1998, he was with the German Aerospace Center (DLR), Oberpfaffenhofen, Germany. From 1991 to 1992, he was on leave at AT&T Bell Laboratories, Murray Hill, NJ. Since 1998 he is a Full Professor of electrical and information engineering at Kiel University, Kiel, Germany. His research interests are in the general area of wireless communications and applied information theory. Since 2014, he has been a Fellow of the IEEE for contributions to decoding and detection that include reliability information.

Jan Sticklus received the Dipl.Ing. degree in electrical engineering from Kiel University of Applied Sciences, Kiel, Germany, in 1993. He is currently working toward the Dr.-Ing. degree at the Faculty of Engineering, University of Kiel, Kiel, Germany. Since then, he has been an Engineer at the GEOMAR Helmholtz Centre for Ocean Research Kiel. From 2007 to 2014, he was a member of the GEOMAR AUV team, working with autonomous underwater vehicles in worldwide deep sea operations. His research interests include optical underwater communications as well as LED and pressure neutral technology.

Andrej Harlakin received the M.Sc. degree in electrical engineering and business administration from Kiel University, Germany, in 2019, where he is currently pursuing the Dr.-Ing. (Ph.D.) degree at the Faculty of Engineering. Since 2019, he has been a Research and Teaching Assistant at the Chair of Information and Coding Theory, Kiel University. His current research interests include underwater optical wireless communications, localization, and radar signal processing.